Electronic Supplementary Information

Manganese Complexes with Chelating and Bridging Di-Triazolylidene Ligands: Synthesis and Reactivity

Sofia Friães,[a] Sara Realista,[a] Clara S. B. Gomes,[b] Paulo N. Martinho,[c] Luís F. Veiros,[d] Martin Albrecht,[e] Beatriz Royo*[a]

Content:

1. Characterisation of **L2a-f** and **1-9** S2
2. Thermogravimetric analysis of complexes **2** and **9** S18
3. Characterisation of **11** S19
4. NMR spectra of the reactions of **2** and **9** with PPh_3 S21
5. Electrochemical studies: CV spectra of **1-10** and FTIR-SEC of **9** S23
6. DFT calculations for **9** S28
7. Crystallographic details of complexes **3**-**5**, **10** and **11** S30
8. FT-IR spectra of the reaction of $Mn(CO)_5Br$ with $KOBu^t$ and $LiOPr^i$ S34

1. Characterisation of ligands **L2a-f** and complexes **1-9**.

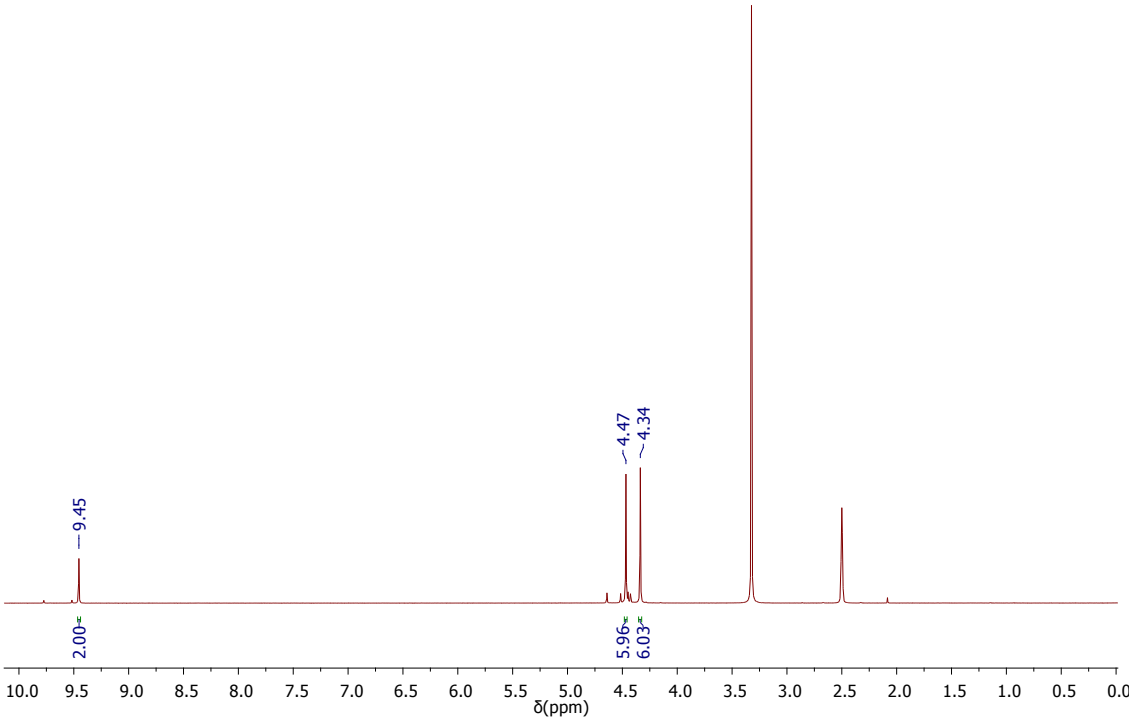

Figure S1. ^{1}H NMR spectrum (DMSO-d_6, 400 MHz) of **L2a**.

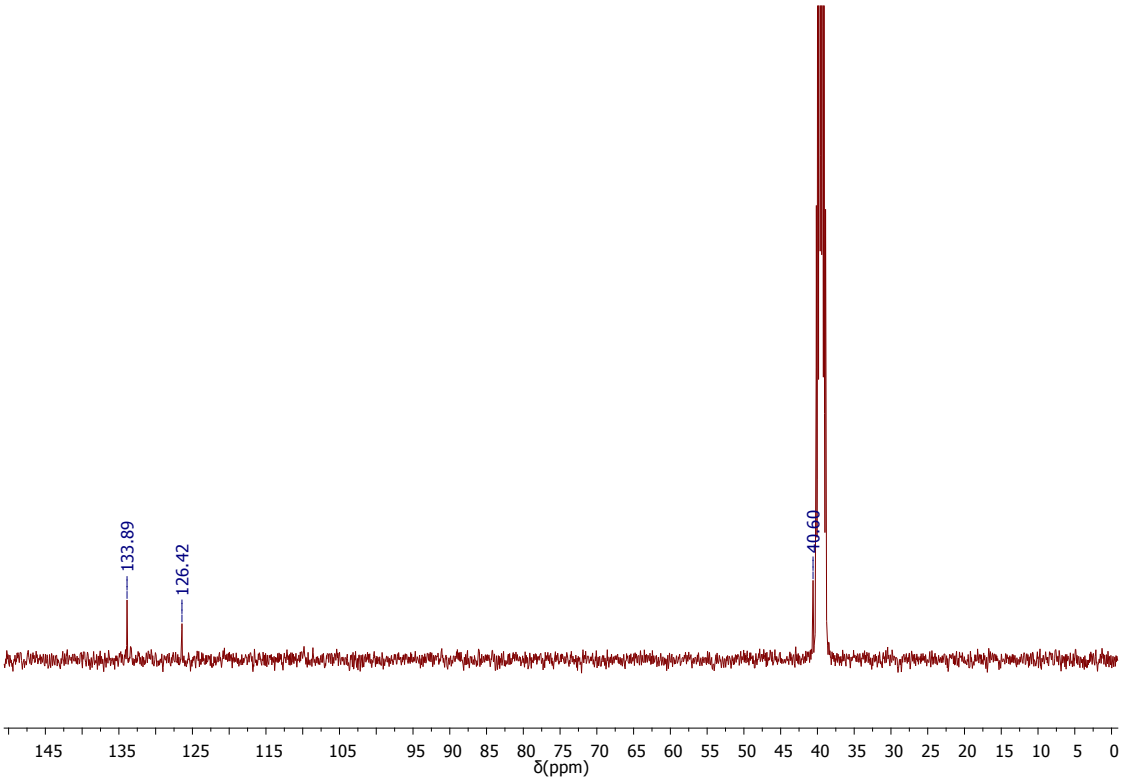

Figure S2. ^{13}C NMR spectrum (DMSO-d_6, 400 MHz) of **L2a**.

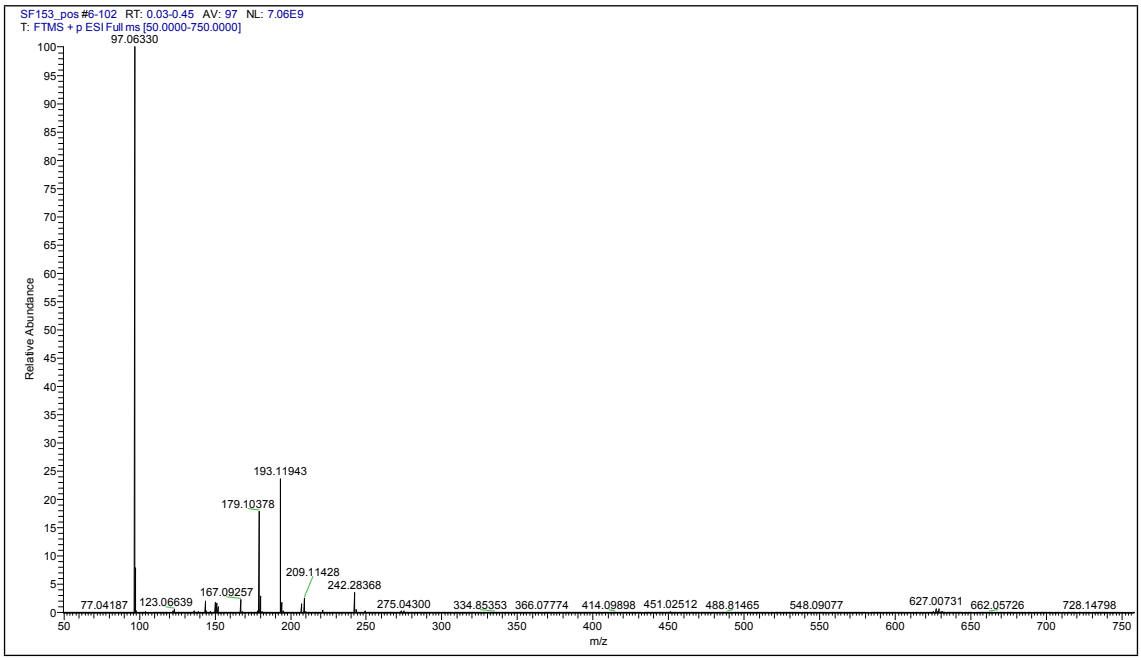

Figure S3. ESI-HRMS of **L2a**.

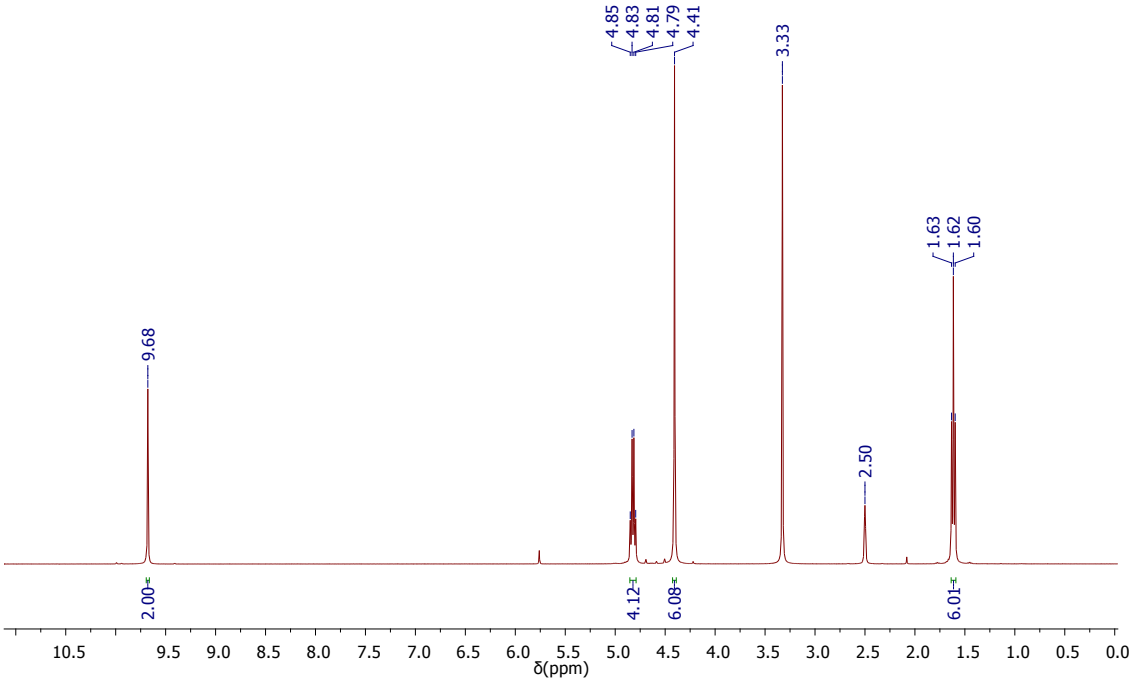

Figure S4. ^{1}H NMR spectrum (DMSO-d_6, 400 MHz) of **L2b**.

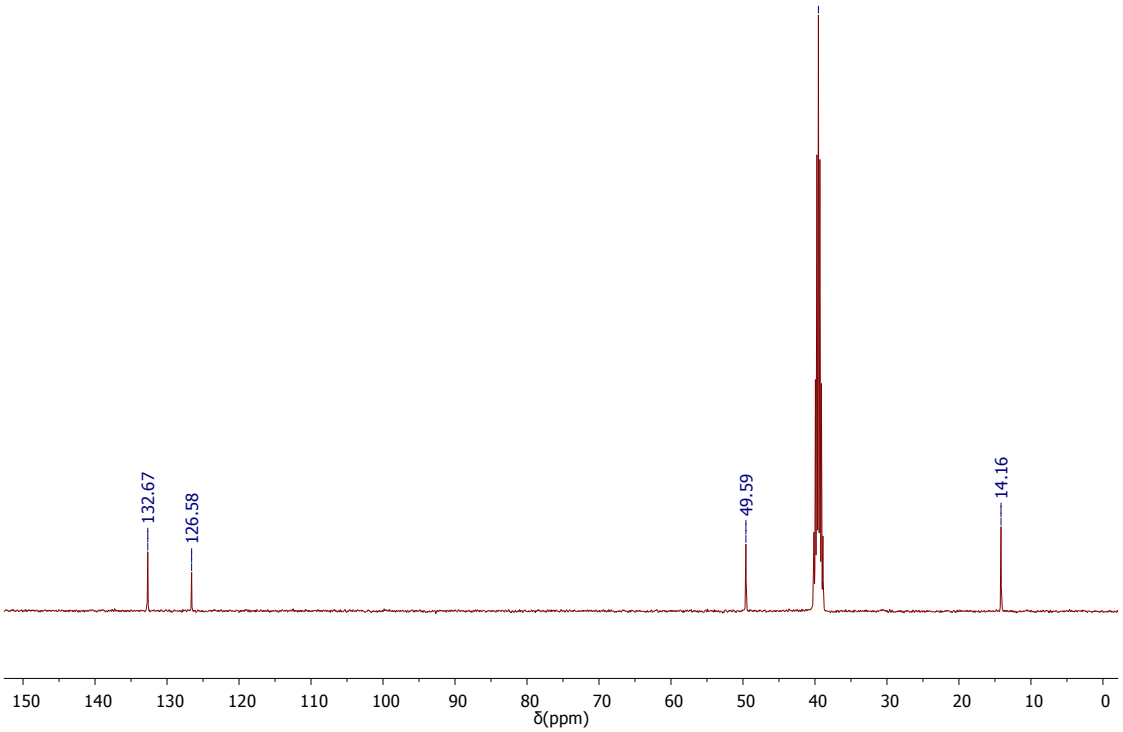

Figure S5. ^{13}C NMR spectrum (DMSO-d_6, 400 MHz) of **L2b**.

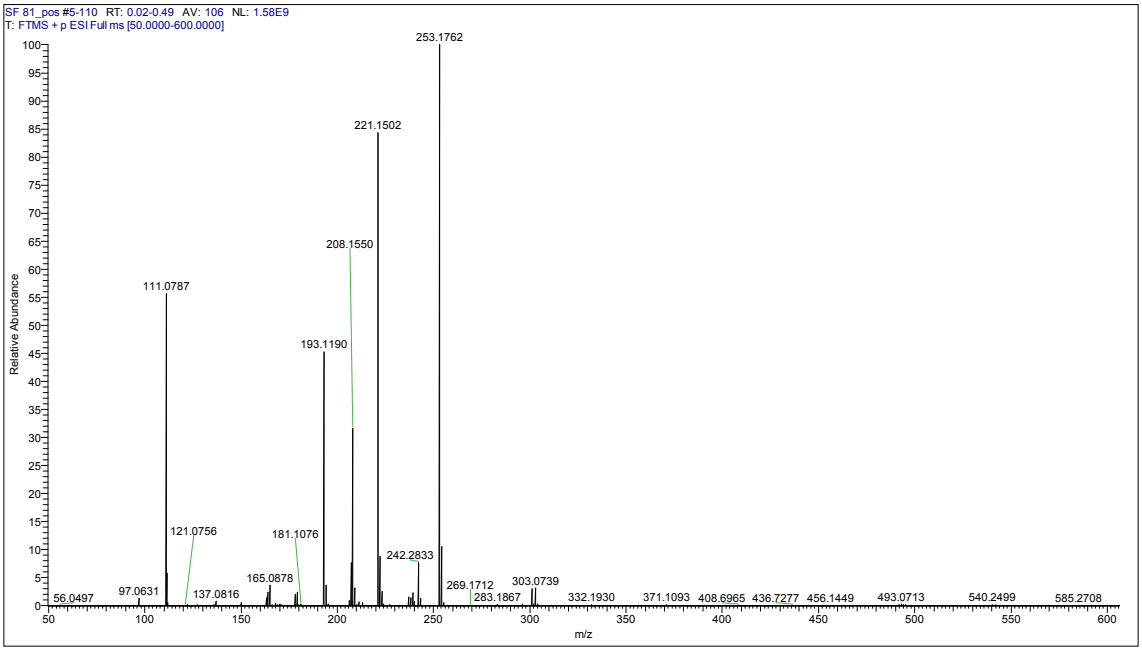

Figure S6. ESI-HRMS Spectrum of **L2b**.

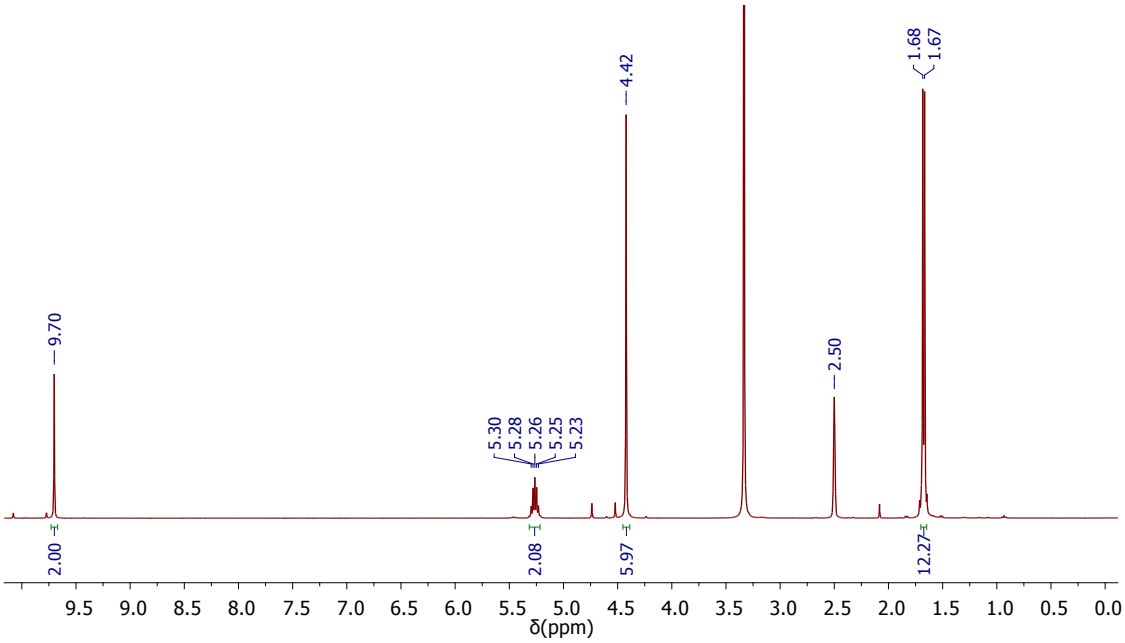

Figure S7. ^{1}H NMR spectrum (DMSO-d_6, 400 MHz) of **L2c**.

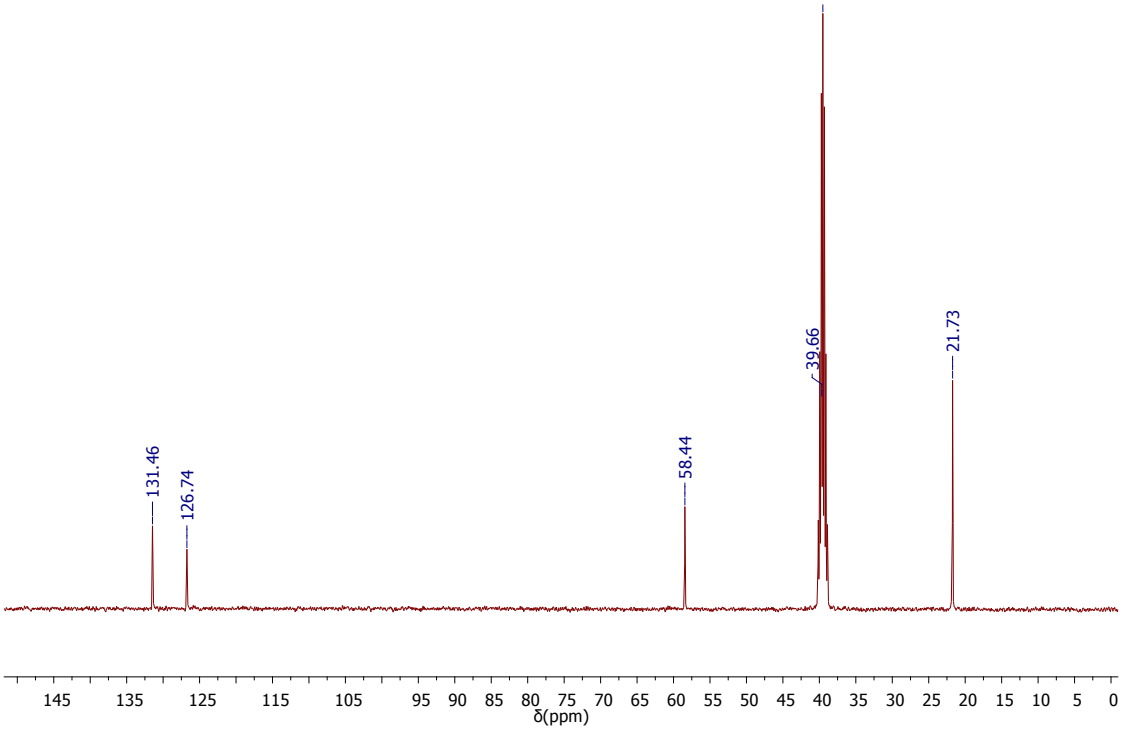

Figure S8. ^{13}C NMR spectrum (DMSO-d_6, 400 MHz) of **L2c**.

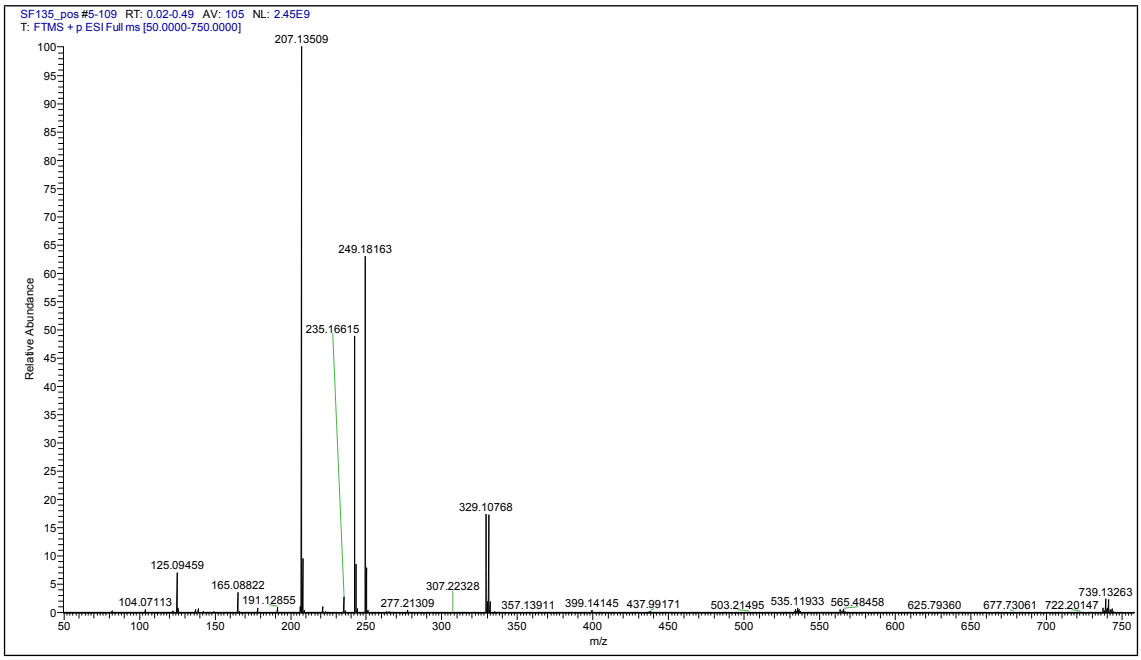

Figure S9. ESI-HRMS Spectrum of **L2c**.

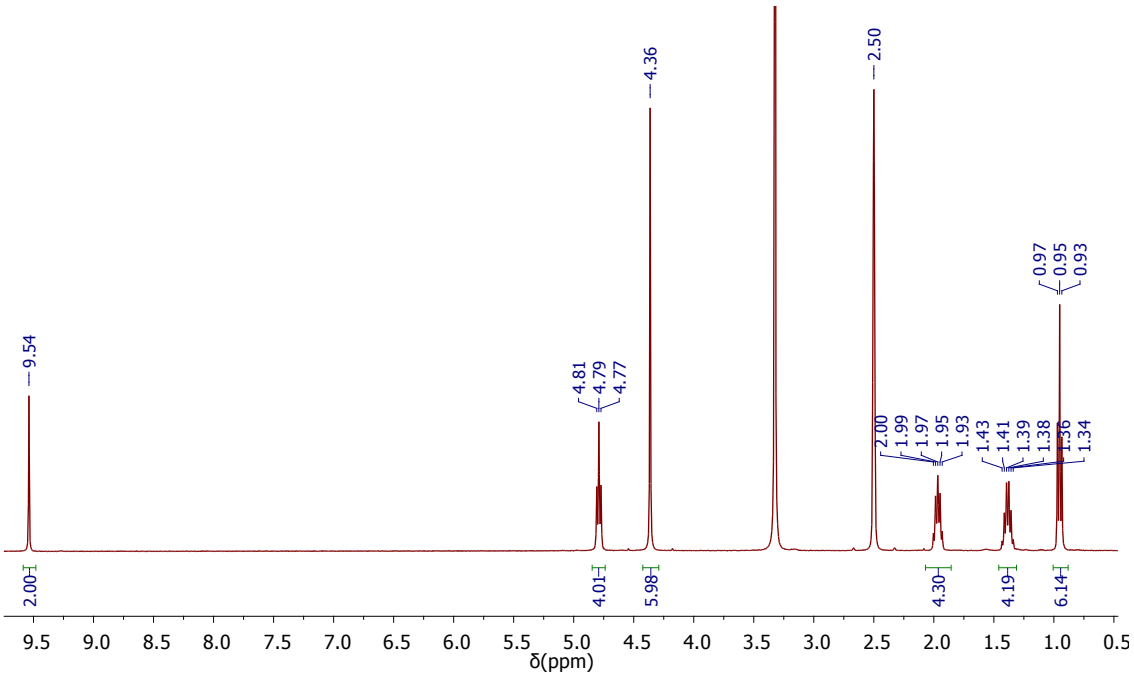

Figure S10. ^{1}H NMR spectrum (DMSO-d_6, 400 MHz) of **L2d**.

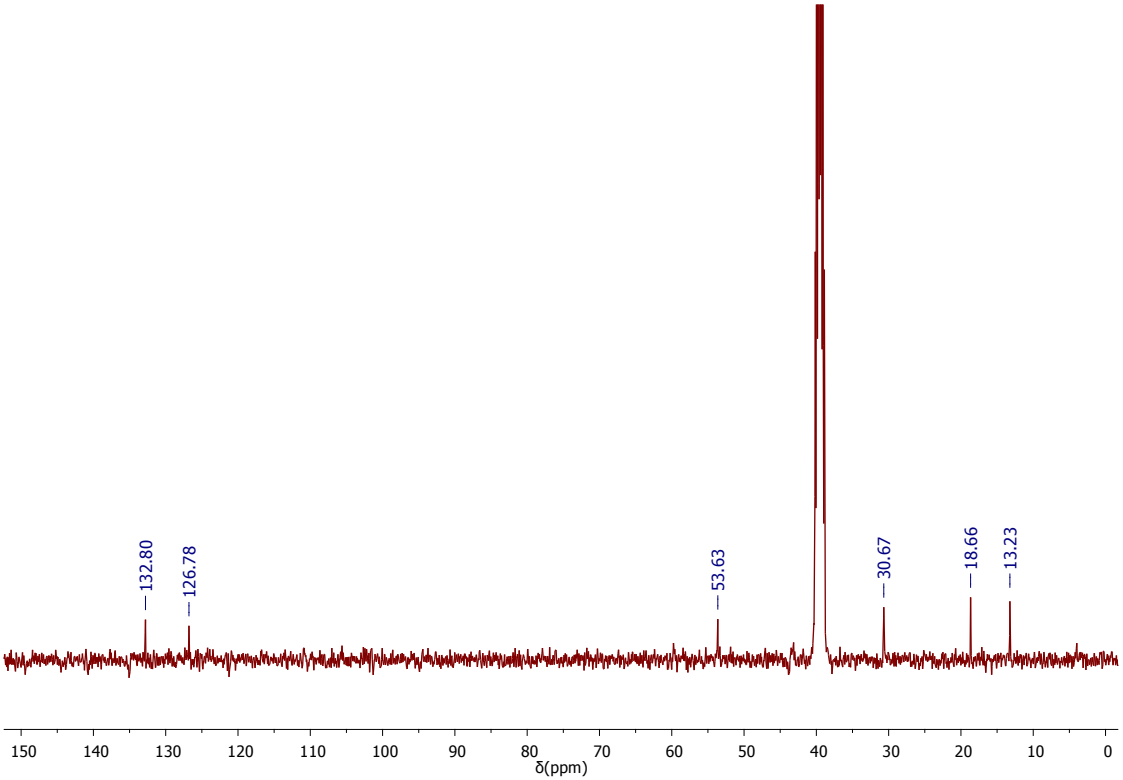

Figure S11. ^{13}C NMR spectrum (DMSO-d_6, 400 MHz) of **L2d**.

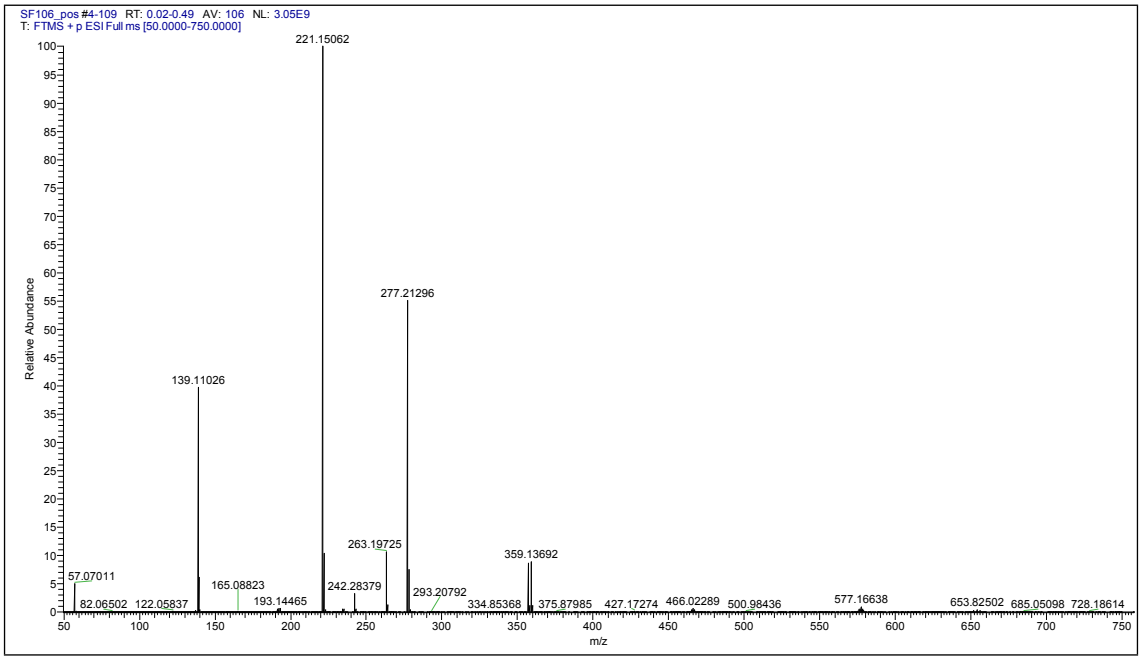

Figure S12. ESI-HRSM Spectrum of **L2d**.

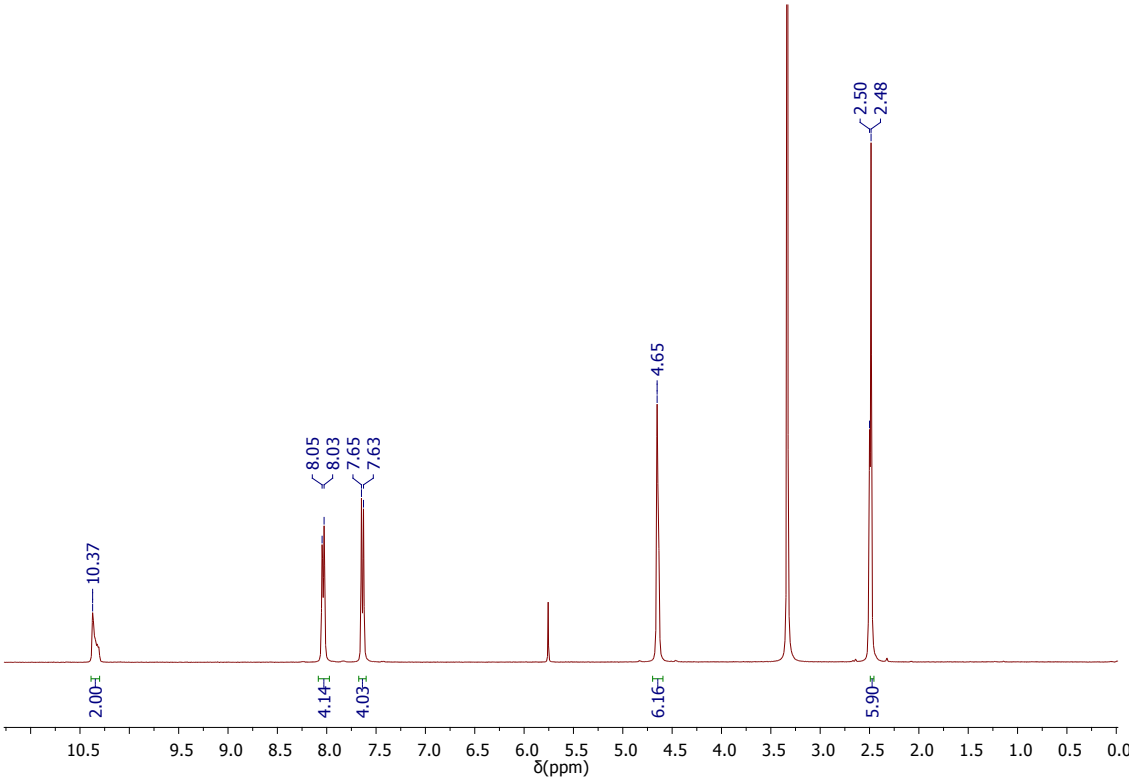

Figure S13. ^{1}H NMR spectrum (DMSO-d_6, 400 MHz) of **L2e**.

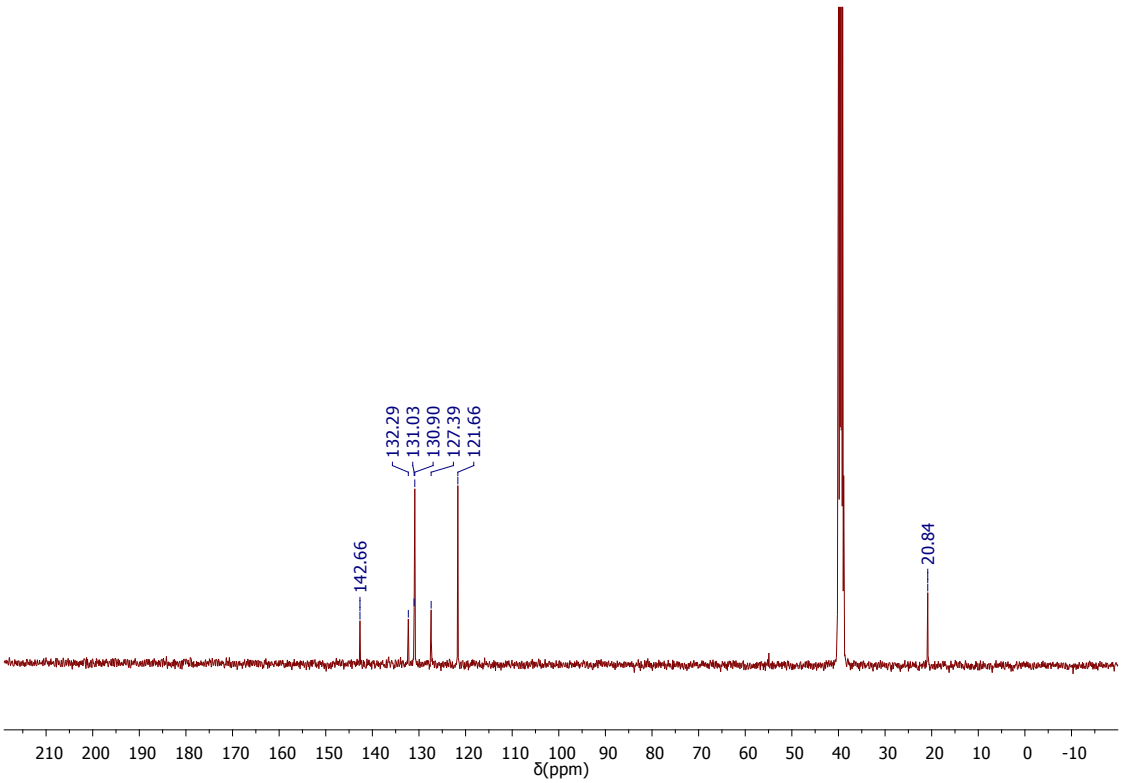

Figure S14. ^{13}C NMR spectrum (DMSO-d_6, 400 MHz) of **L2e**.

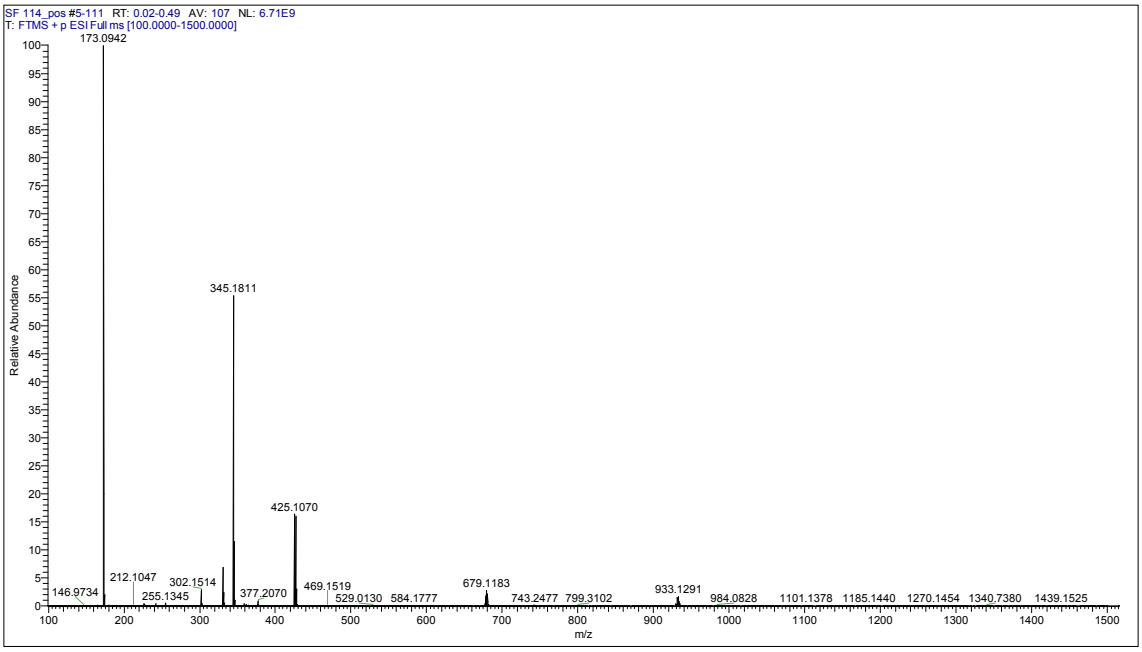

Figure S15. ESI-HRMS Spectrum of **L2e**.

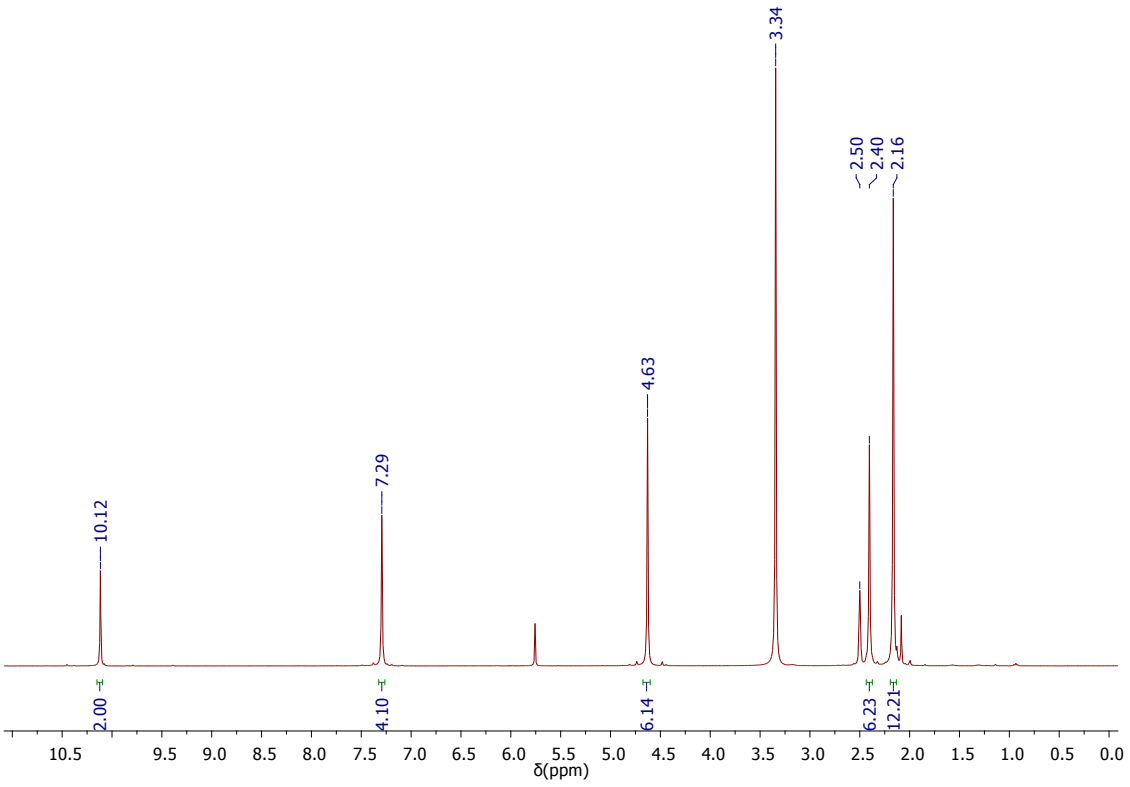

Figure S16. ^{1}H NMR spectrum (DMSO-d_6, 400 MHz) of **L2f**.

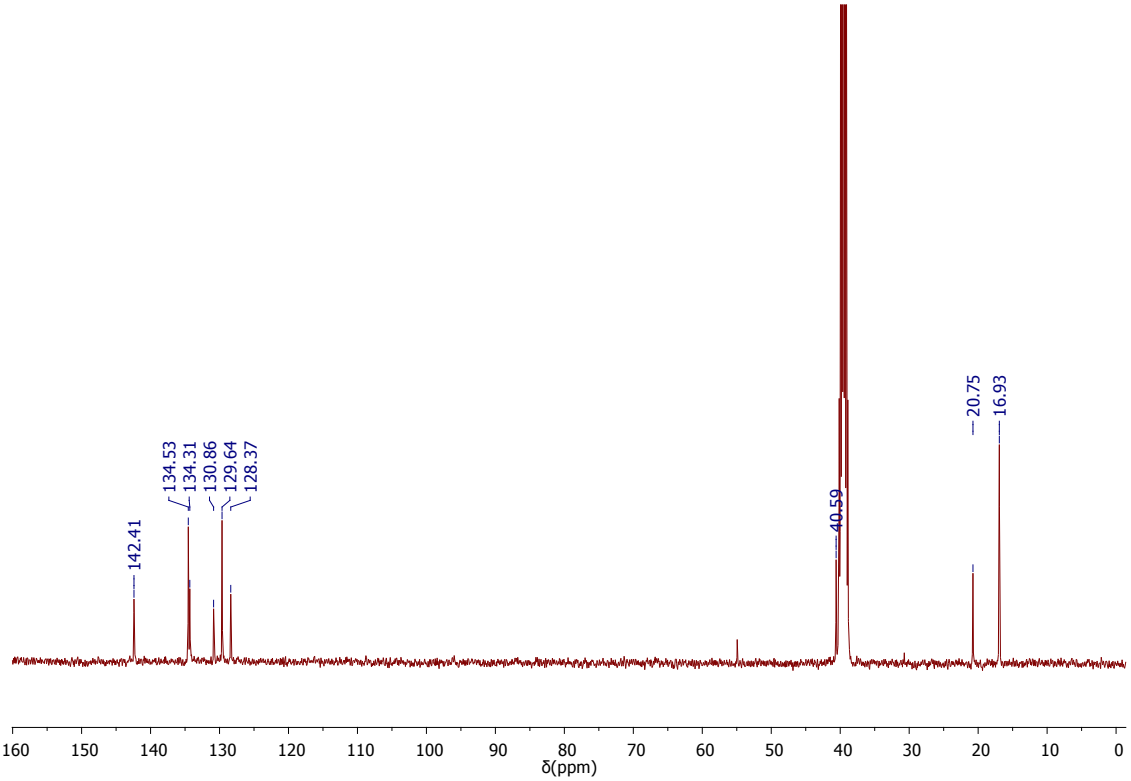

Figure S17 ^{13}C NMR spectrum (DMSO-d_6, 400 MHz) of **L2f**.

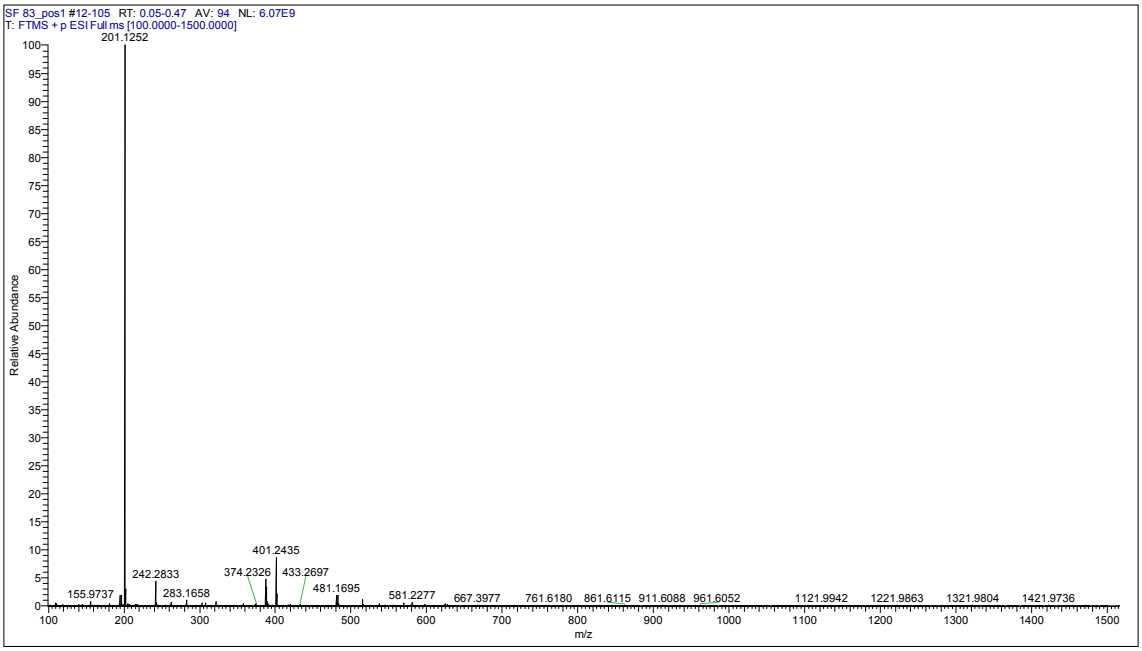

Figure S18 ESI-HRMS Spectrum of **L2f**.

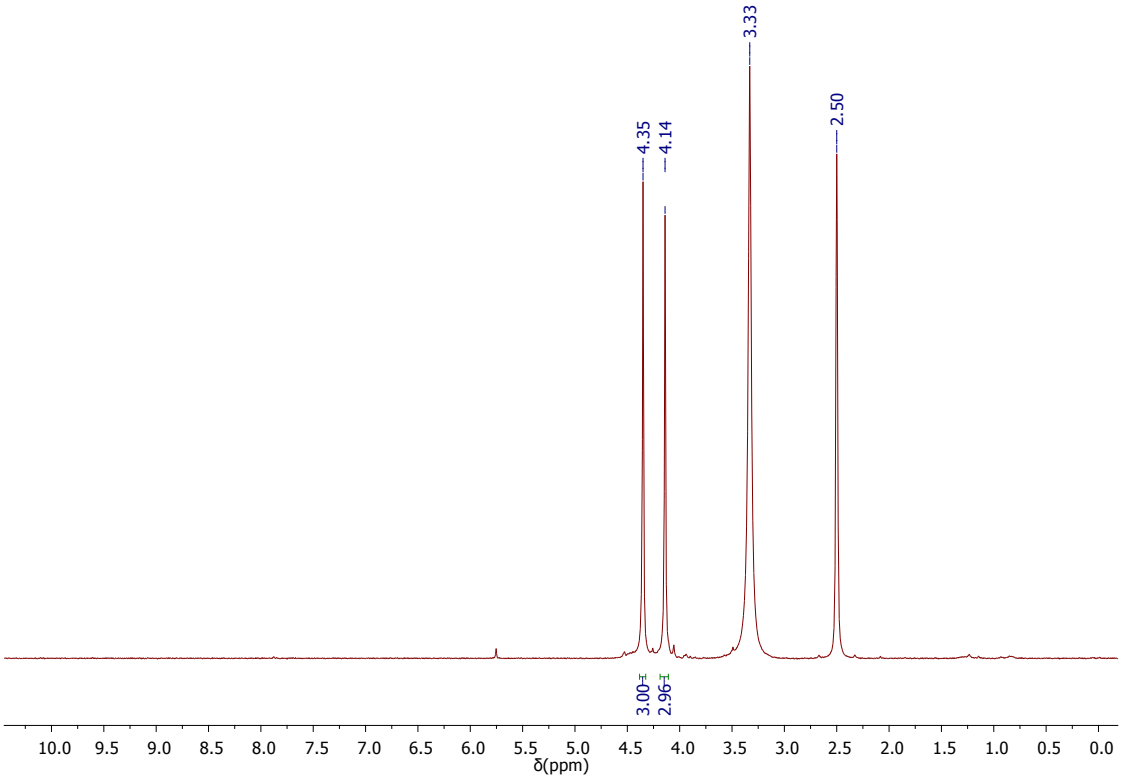

Figure S19. ^{1}H NMR spectrum (DMSO-d_6, 400 MHz) of **1**.

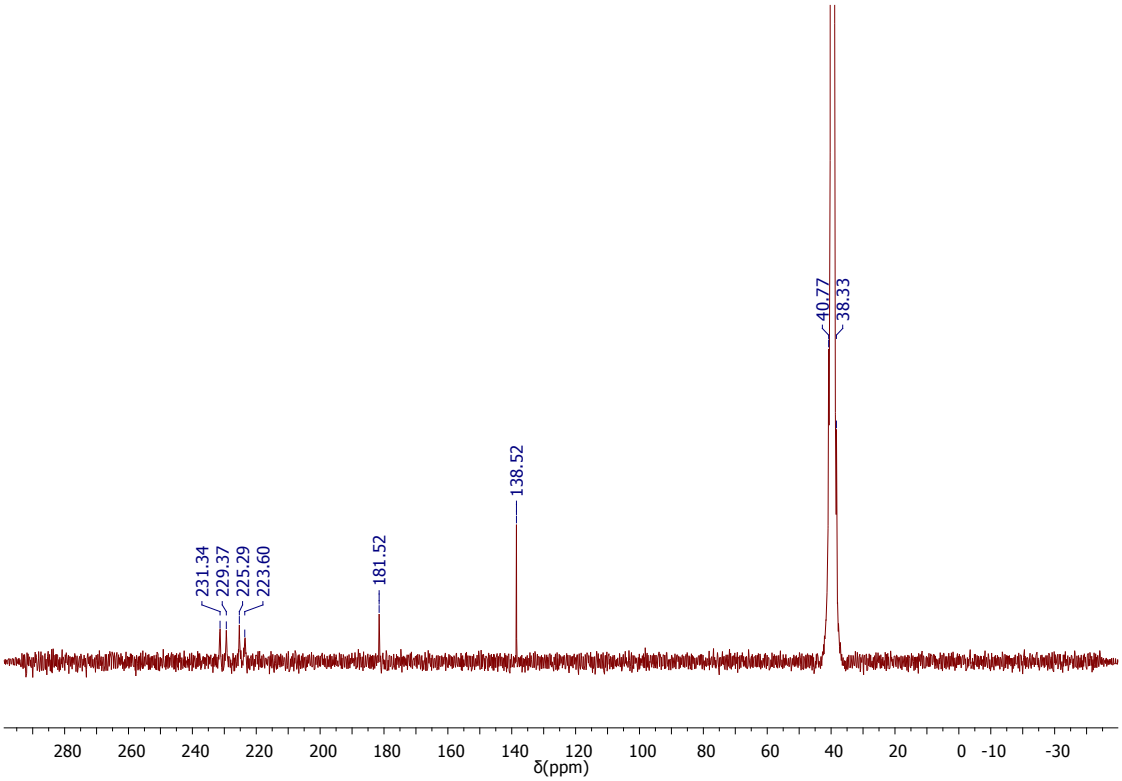

Figure S20. ^{13}C NMR spectrum (DMSO-d_6, 500 MHz) of **1**.

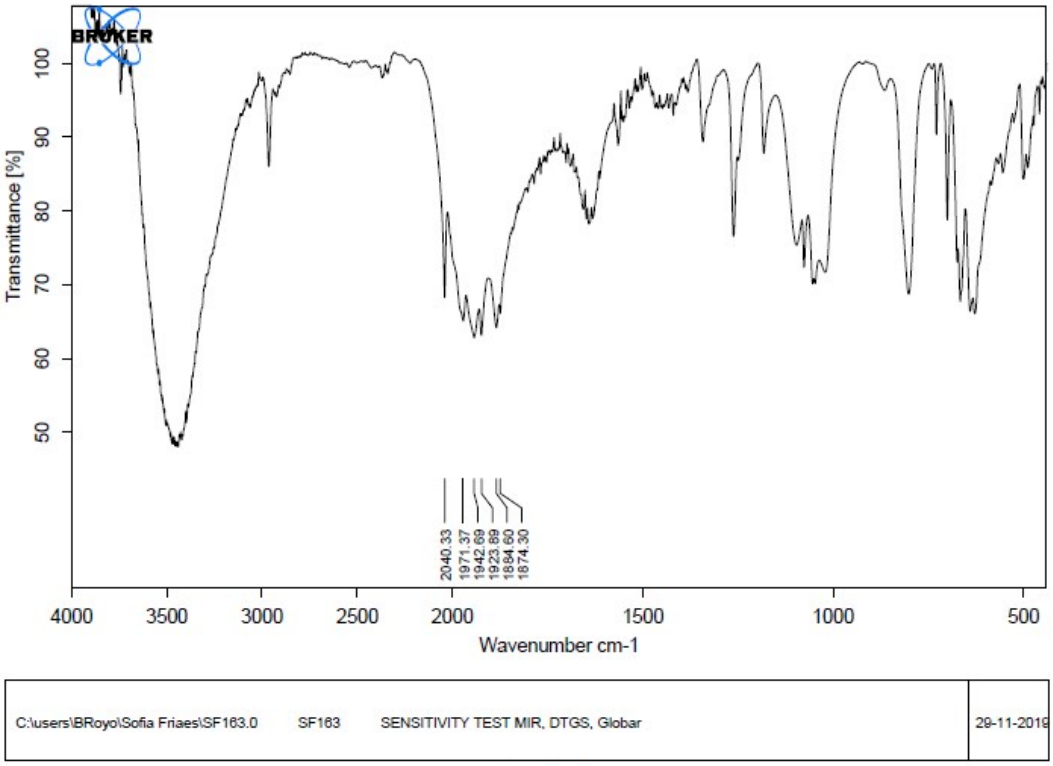

Figure S21. IR spectrum of **1** in KBr.

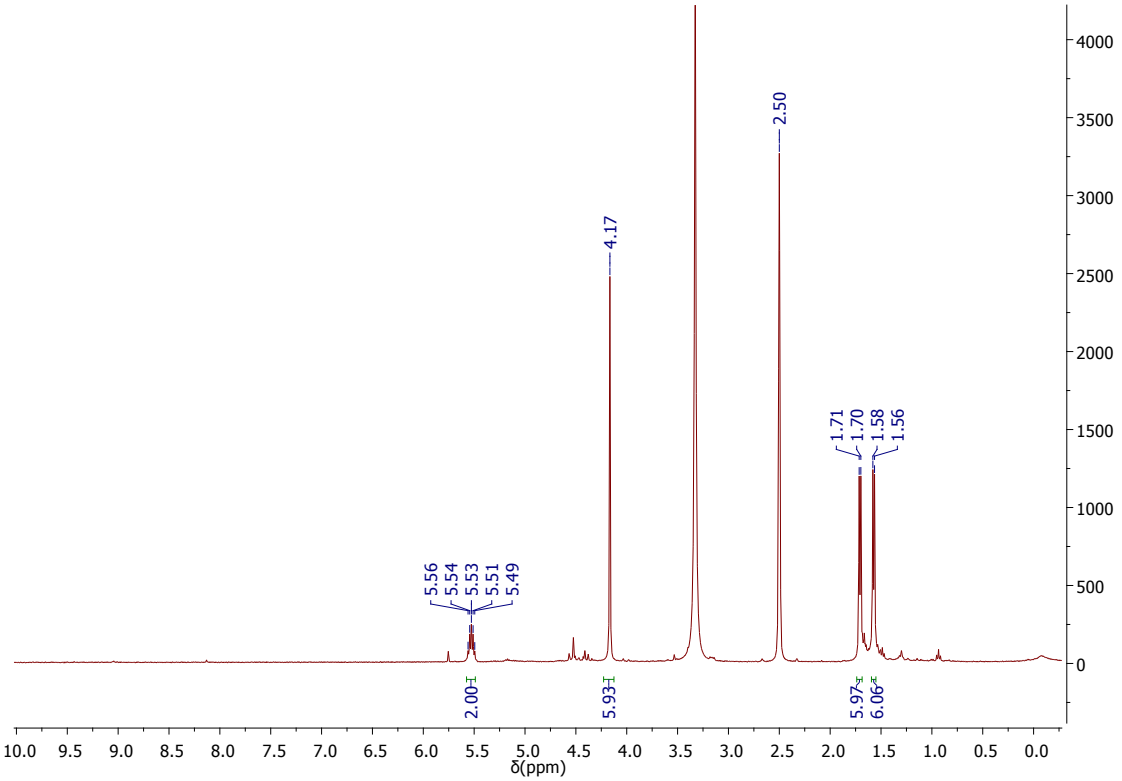

Figure S22. ^{1}H NMR spectrum (DMSO-d_6, 400 MHz) of **3**.

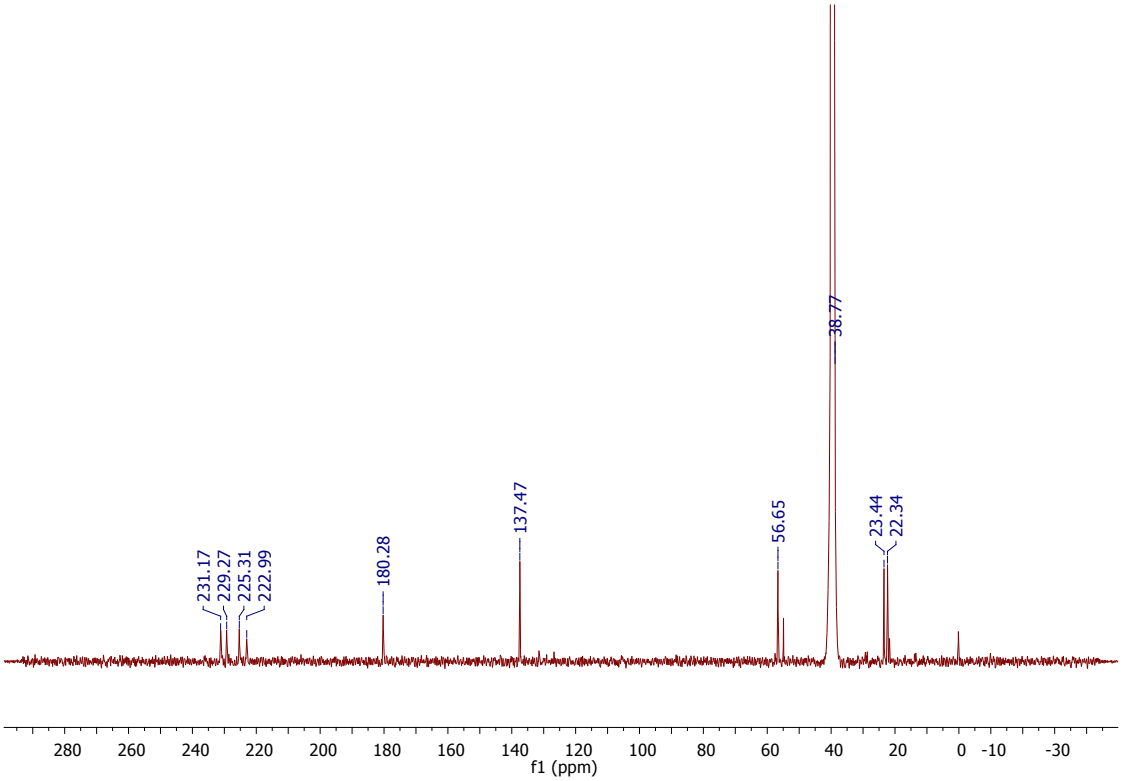

Figure S23. ^{13}C NMR spectrum (DMSO-d_6, 500 MHz) of **3**.

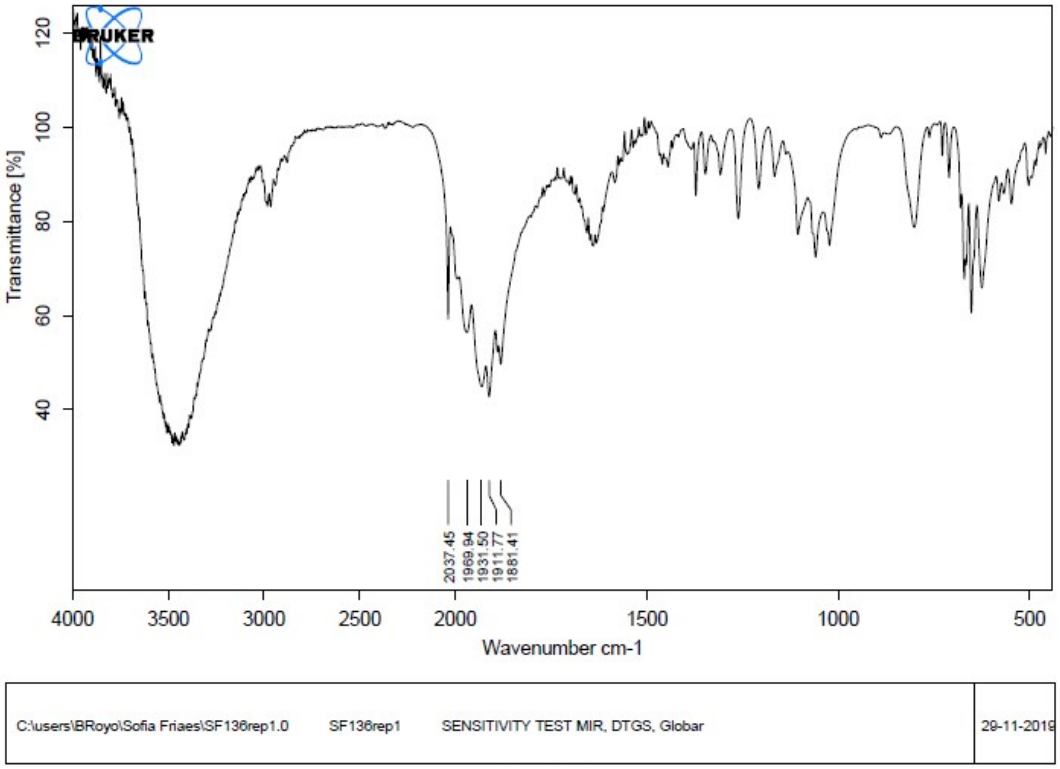

Figure S24. IR spectrum of **3** in KBr.

(a)

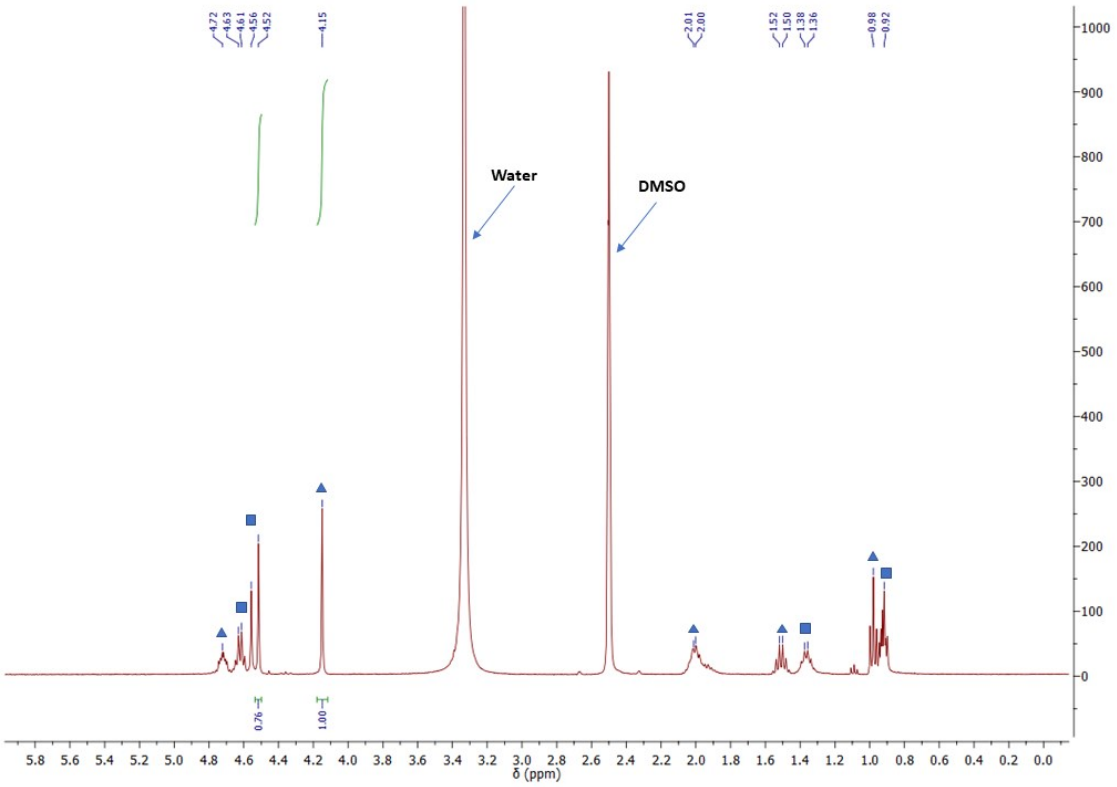
4.72
4.63
4.61
4.56
4.52
4.15
2.01
2.00
1.52
1.50
1.38
1.36
0.98
0.92
Water
DMSO
0.76
1.00
δ (ppm)

(b)

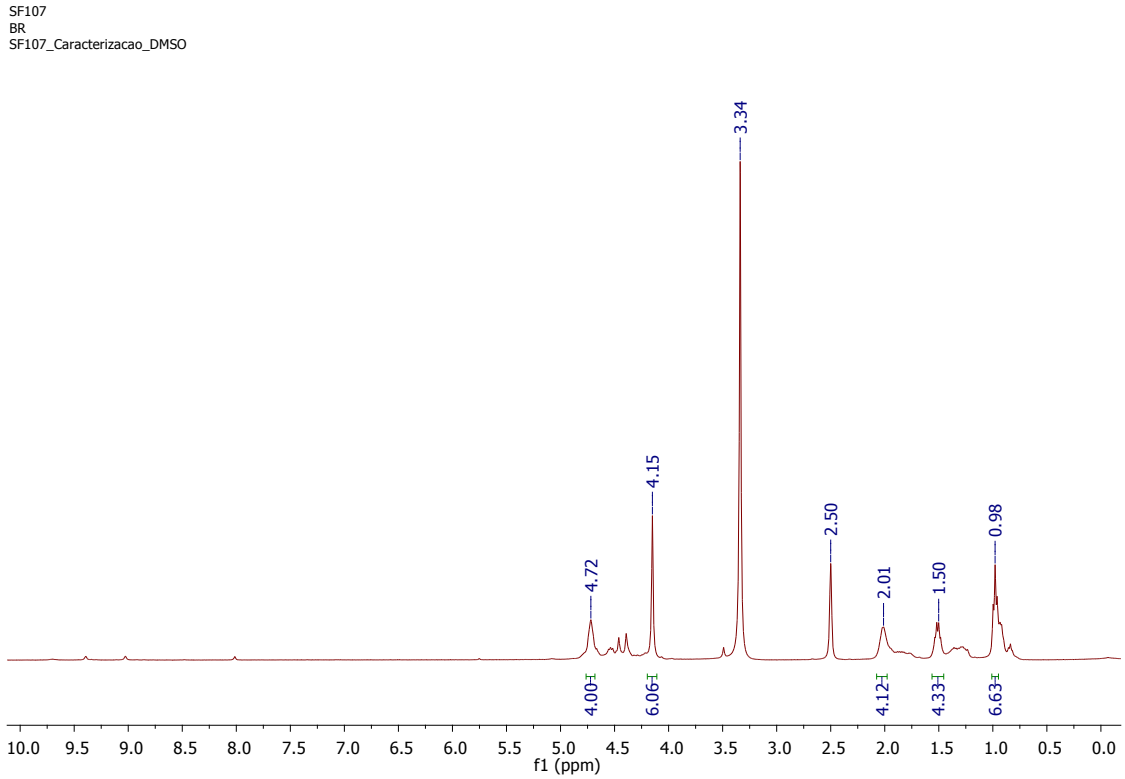
SF107
BR
SF107_Caracterizacao_DMSO
3.34
4.15
4.72
2.50
2.01
1.50
0.98
4.00
6.06
4.12
4.33
6.63
f1 (ppm)

(c)

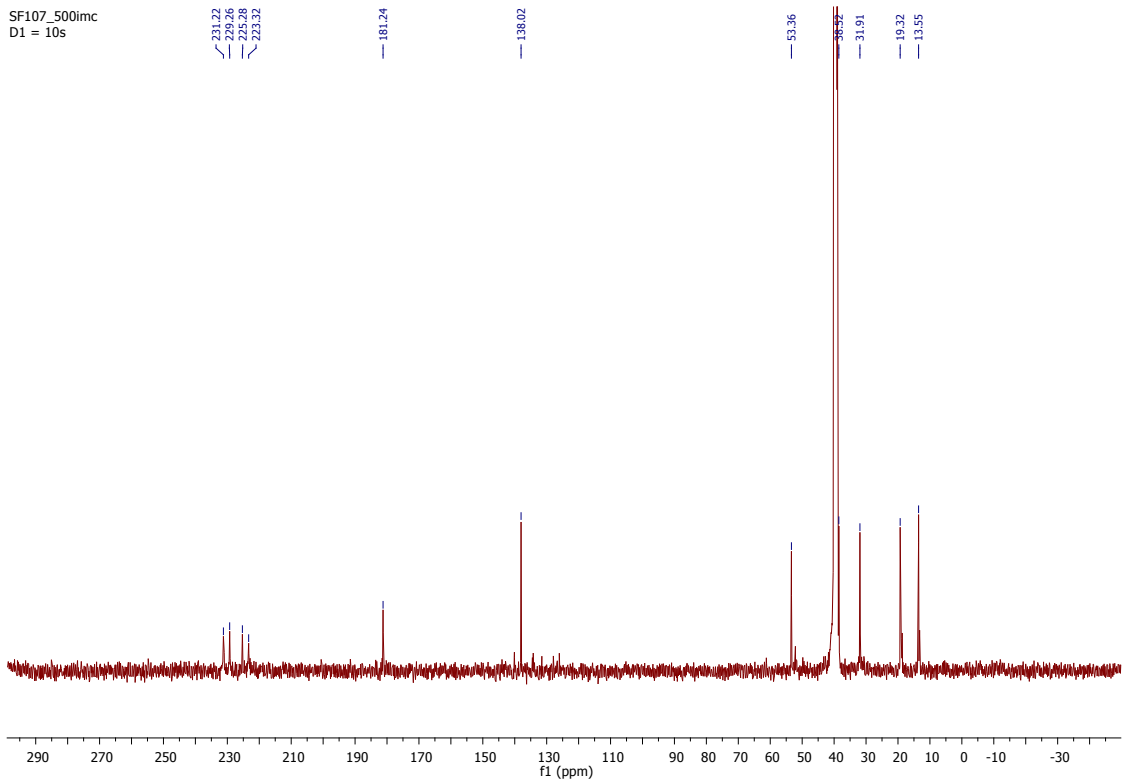

Figure S25. (a) ^{1}H NMR spectrum (DMSO-d_6, 400 MHz) of the mixture of **4** and **6**, where blue triangle corresponds to dimetallic complex **4** and blue square indicates monometallic complex **6**; (b) ^{1}H NMR spectrum (DMSO-d_6, 400 MHz) of **4**; (c) ^{13}C NMR spectrum (DMSO-d_6, 125 MHz) of **4**.

(a)

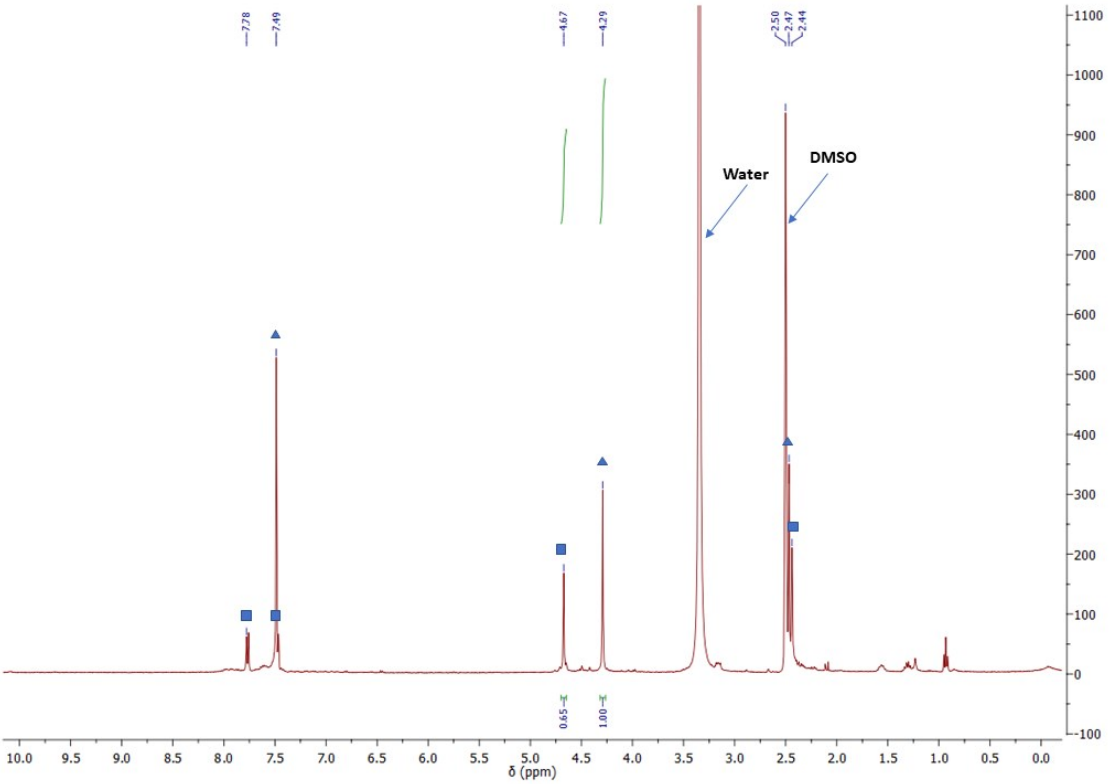
7.78
7.49
4.67
4.29
2.50
2.47
2.44
Water
DMSO
0.65
1.00
δ (ppm)

(b)

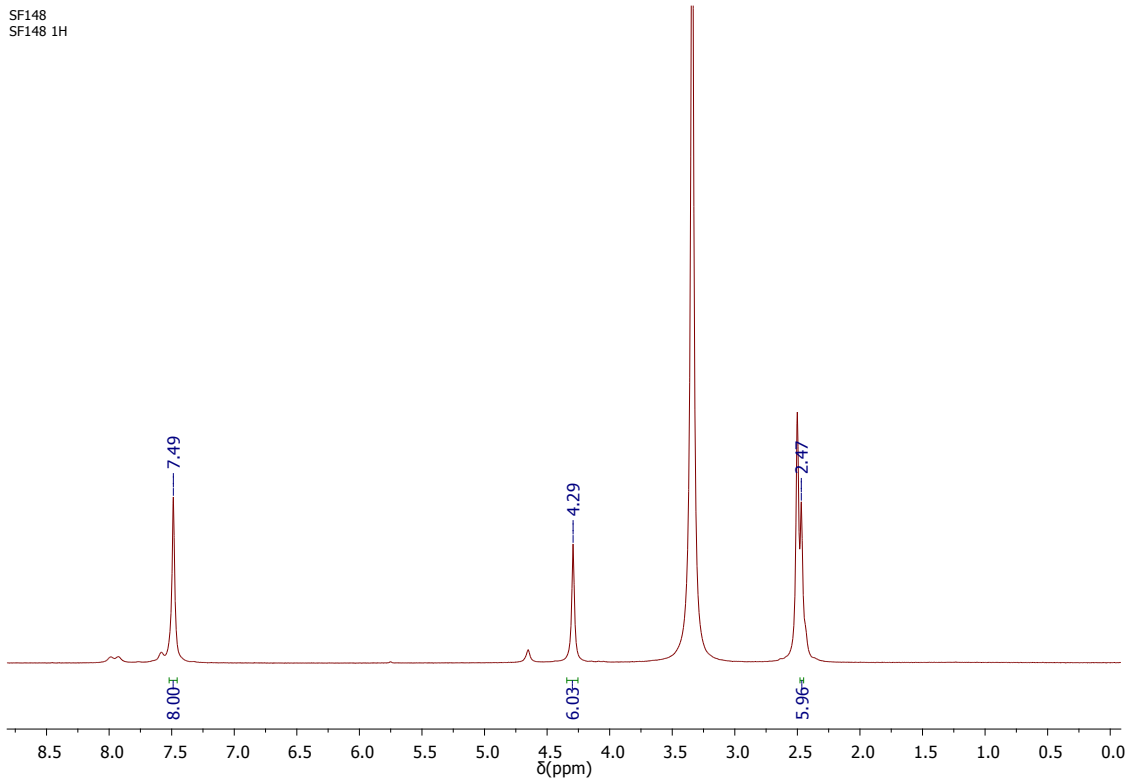
SF148
SF148 1H
7.49
4.29
2.47
8.00
6.03
5.96
δ(ppm)

(c)

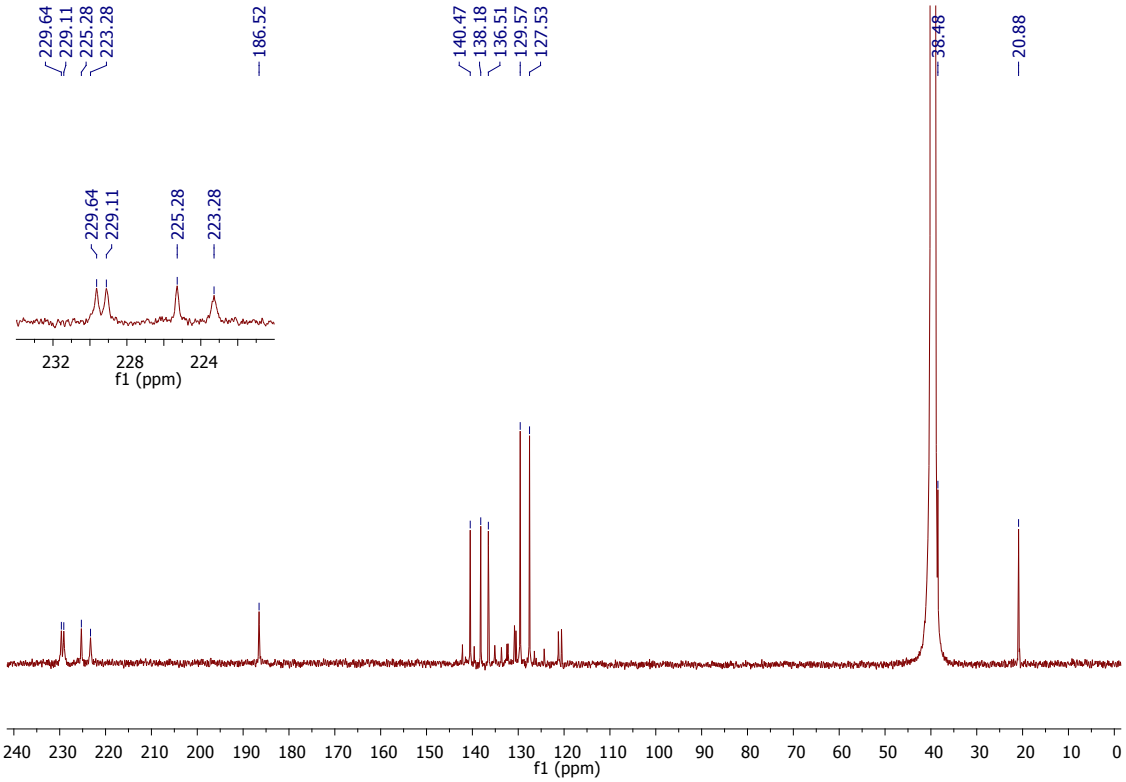

Figure S26. (a) ^{1}H NMR spectrum (DMSO-d_6, 400 MHz) of the mixture of **5** and **7**, where blue triangle corresponds to dimetallic complex **5** and blue square indicates monometallic complex **7.** (b) ^{1}H NMR spectrum (DMSO-d_6, 400 MHz) of **5**; (c) ^{13}C NMR spectrum (DMSO-d_6, 125 MHz) of **5**.

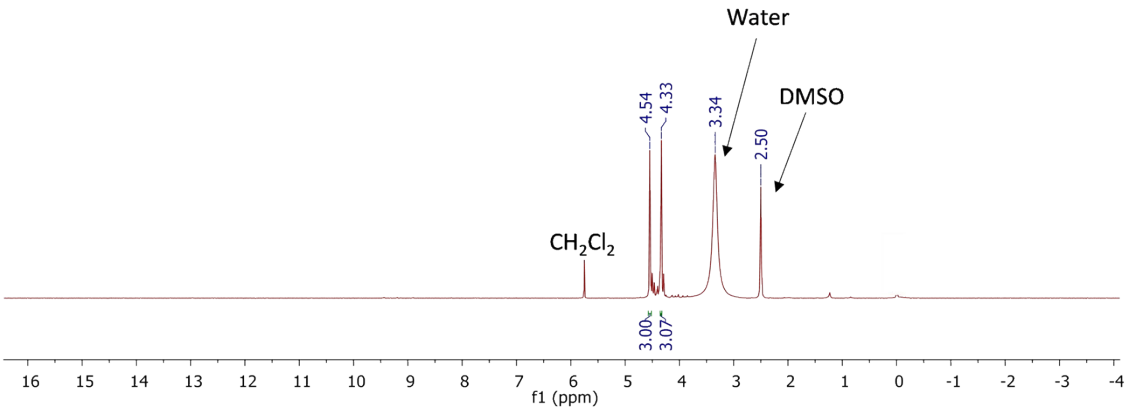

Figure S27. ^{1}H NMR spectrum (DMSO-d_6, 400 MHz) of **8.**

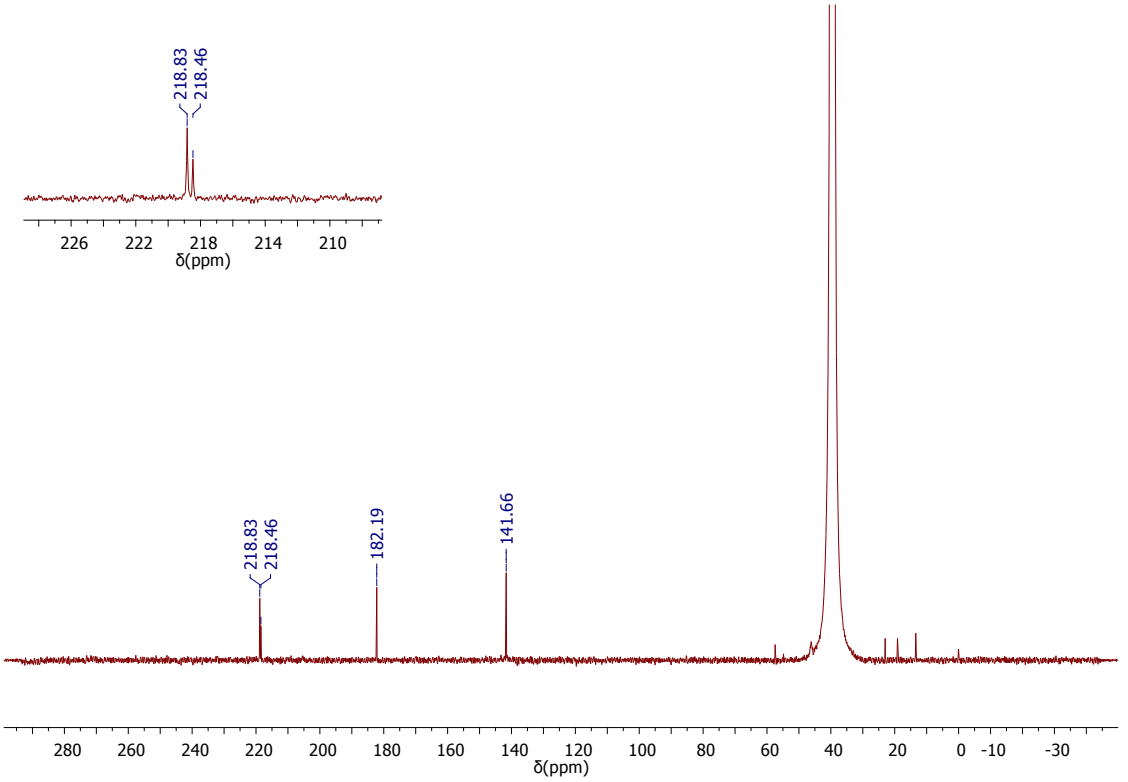

Figure S28. ^{13}C NMR spectrum (DMSO-d_6, 500 MHz) of **8.**

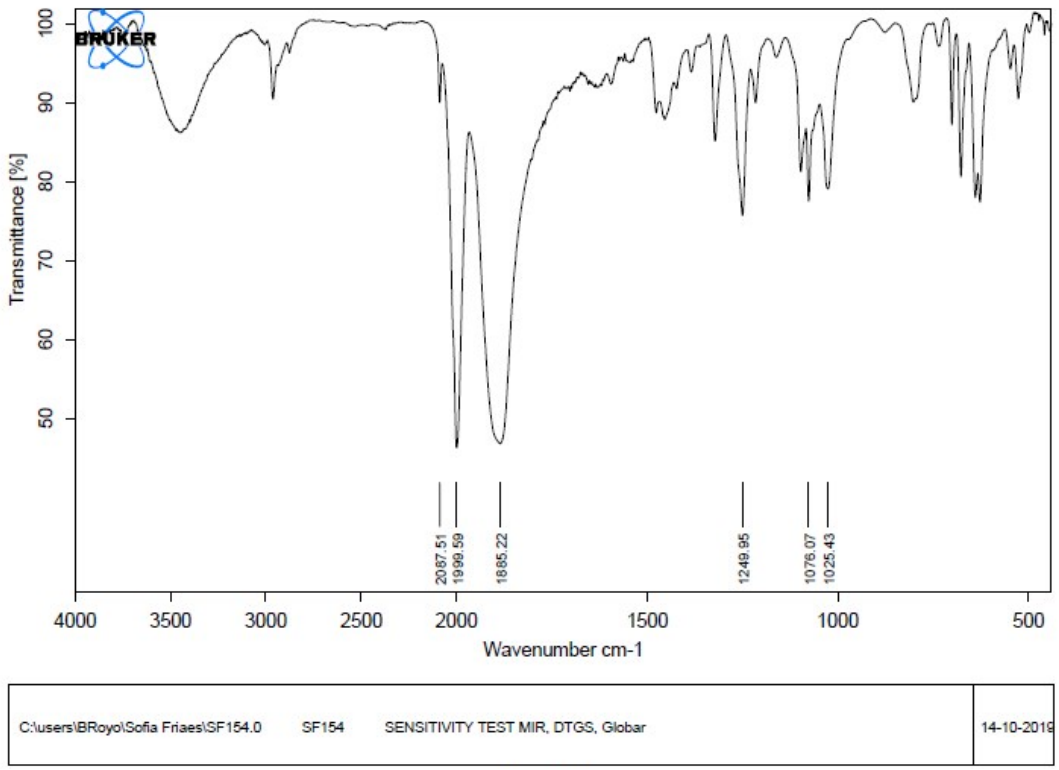

Figure S29. IR spectrum of **8** in KBr.

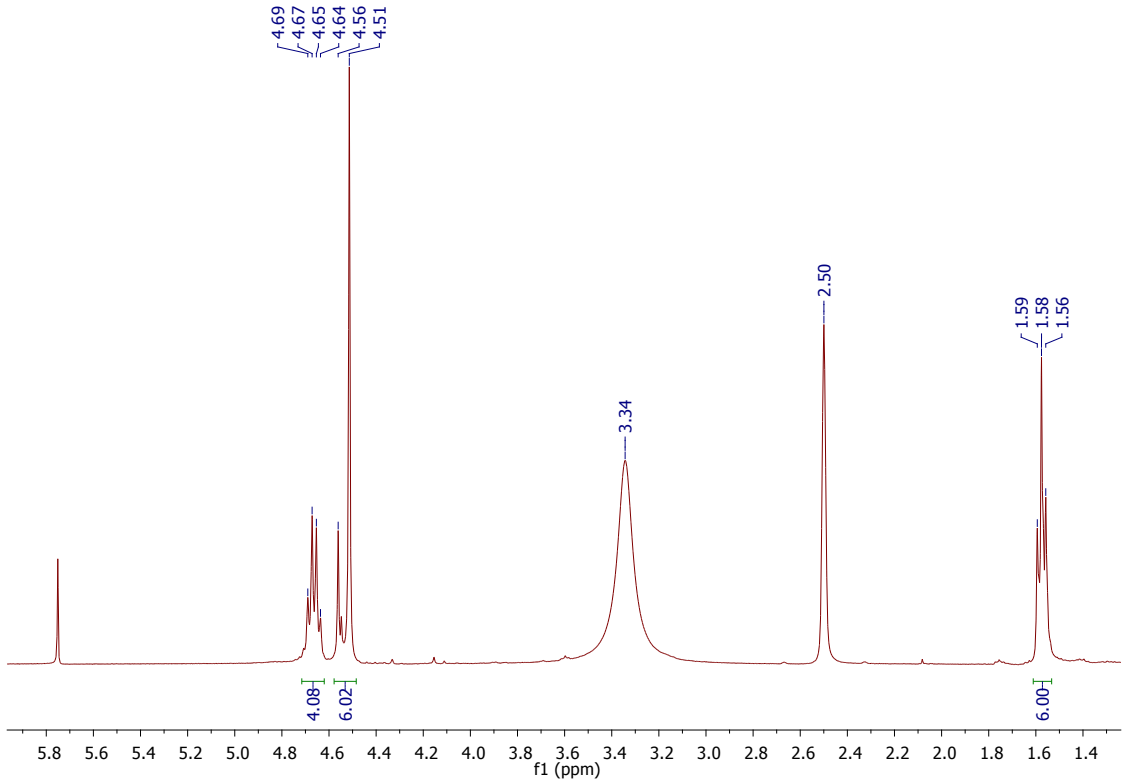

Figure S30. ^{1}H NMR spectrum (DMSO-d_6, 400 MHz) of **9.**

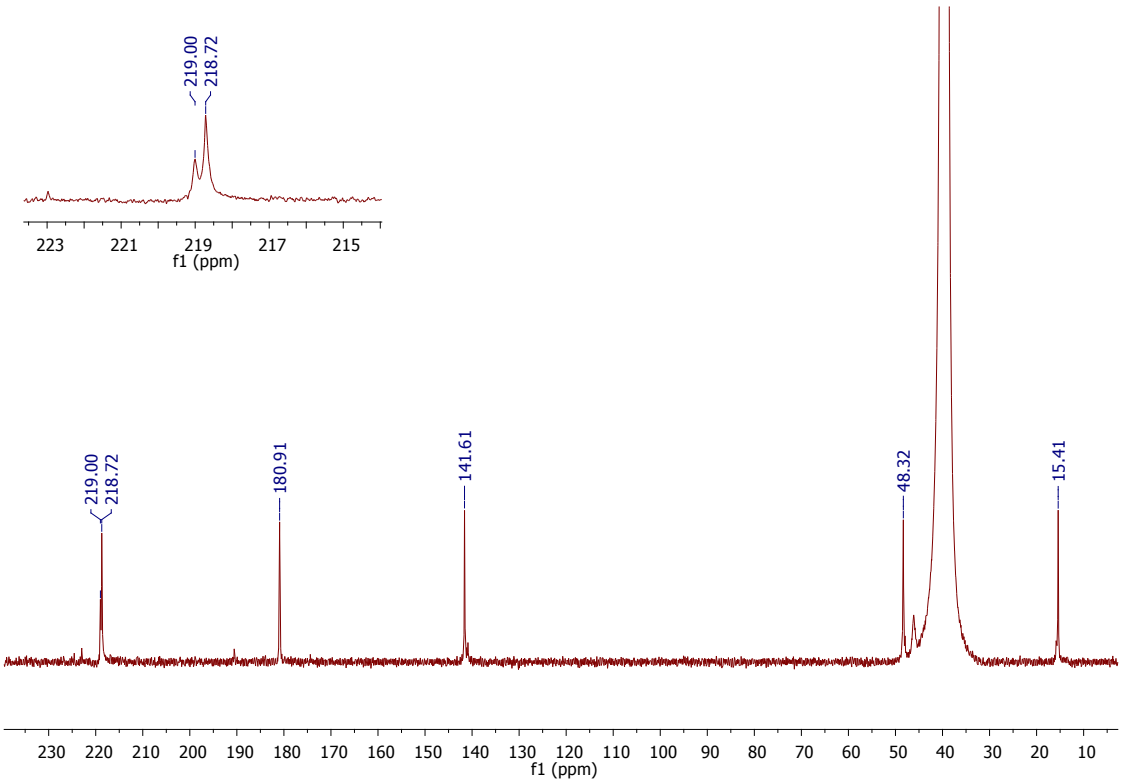

Figure S31. ^{13}C NMR spectrum (DMSO-d_6, 500 MHz) of **9.**

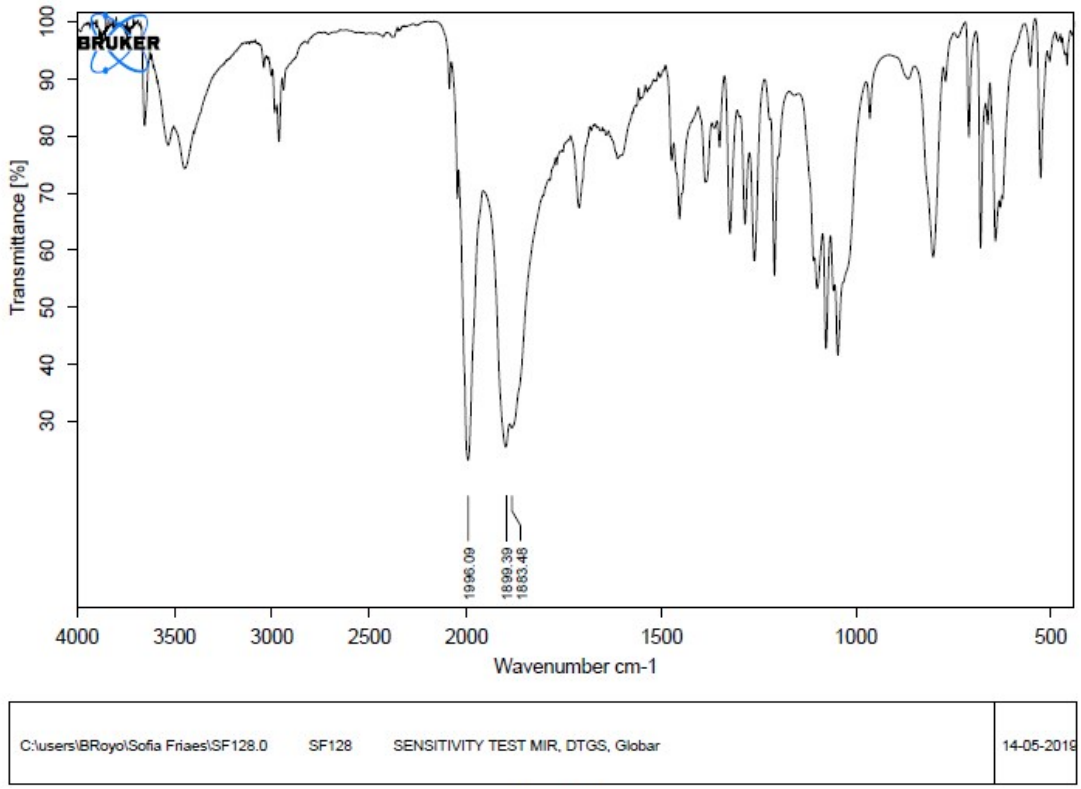

Figure S32. IR spectrum of **9** in KBr.

2. Thermogravimetric analysis of complexes **2** and **9**

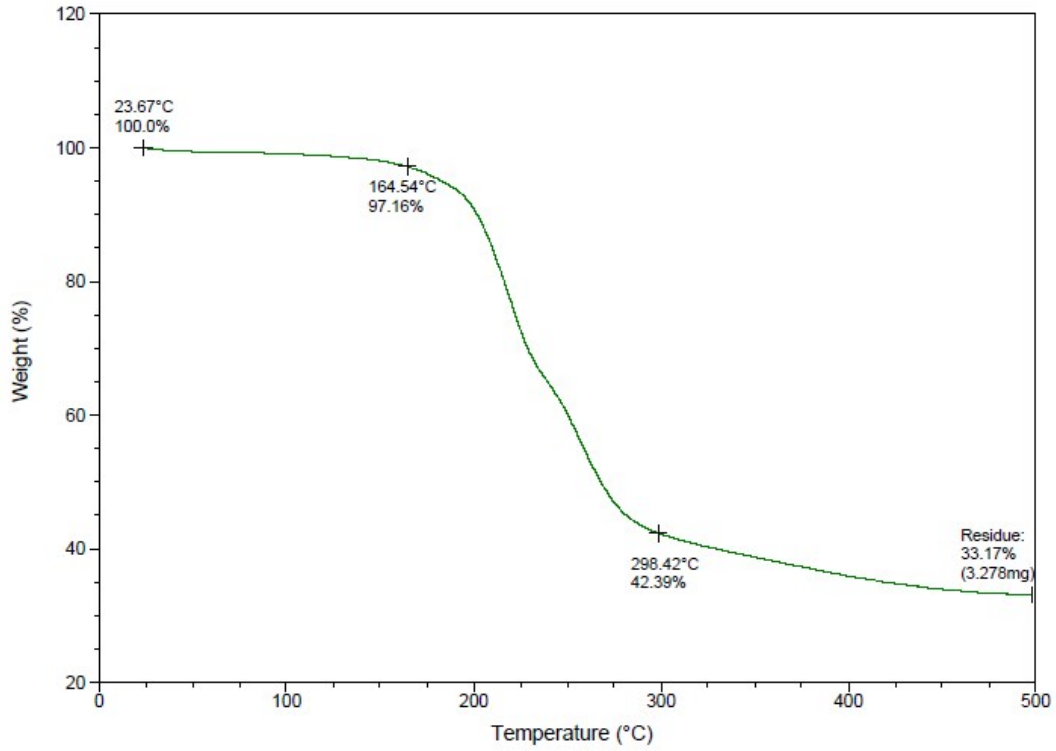

Figure S33. Thermogram of complex **2**.

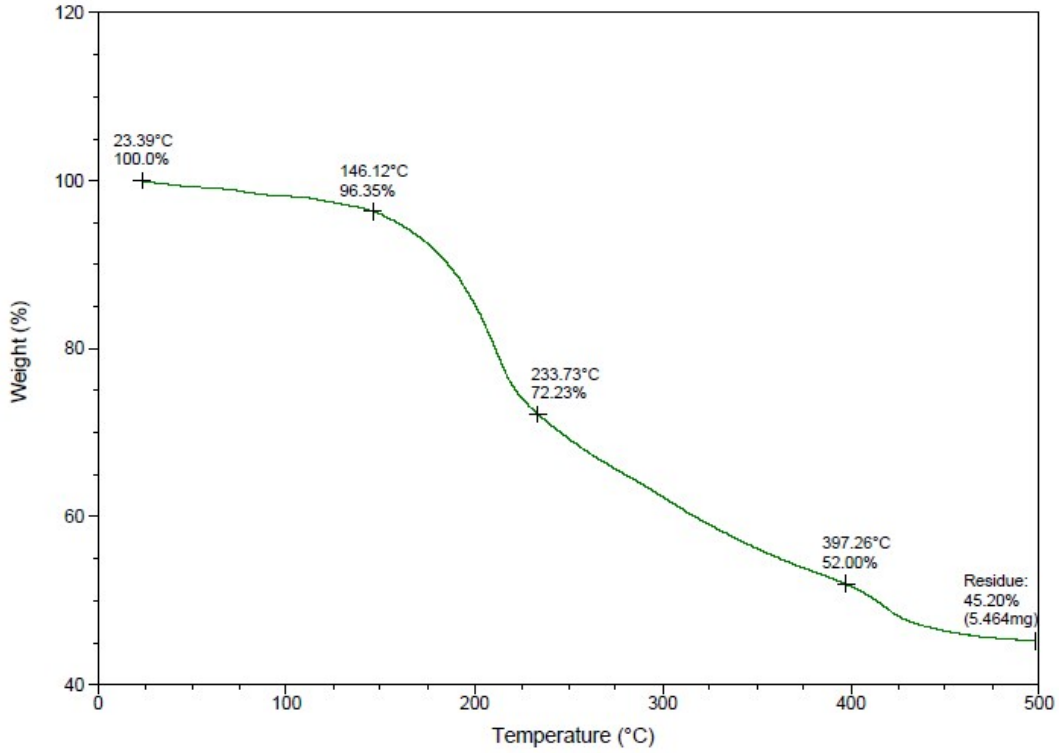

Figure S34. Thermogram of complex **9**.

3. Characterisation of complex **11**.

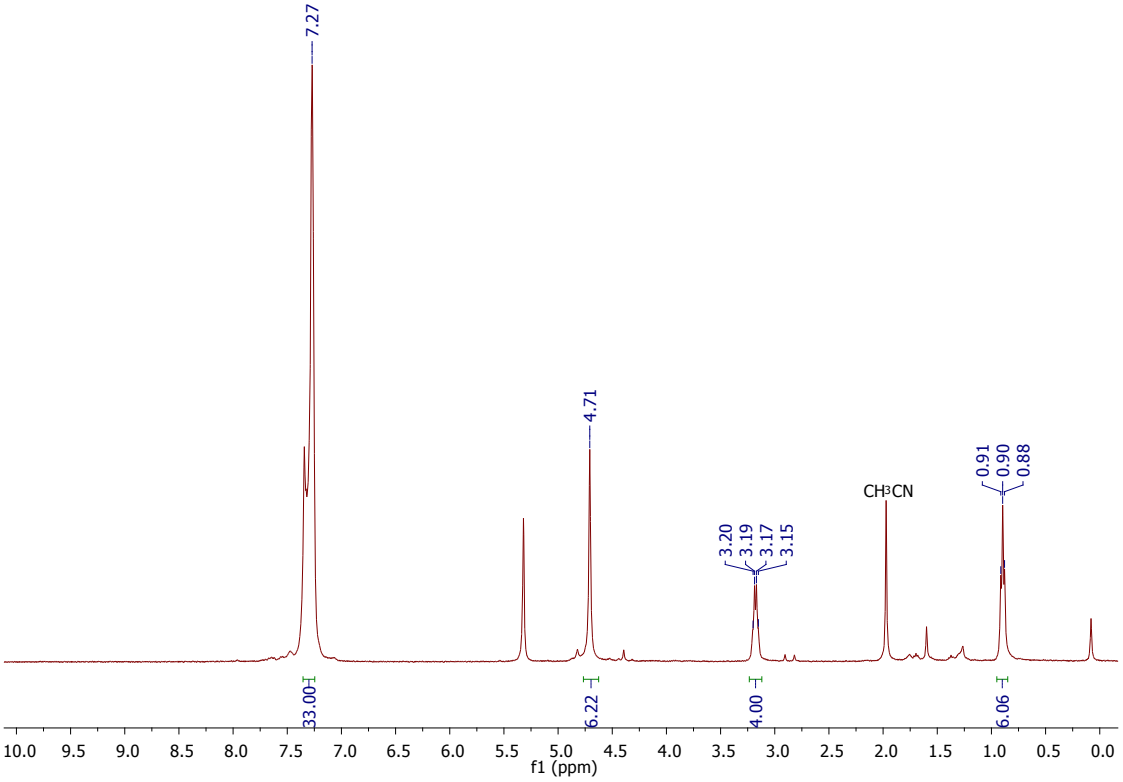

Figure S35. ^{1}H NMR (CD_2Cl_2, 400 MHz) of complex **11**.

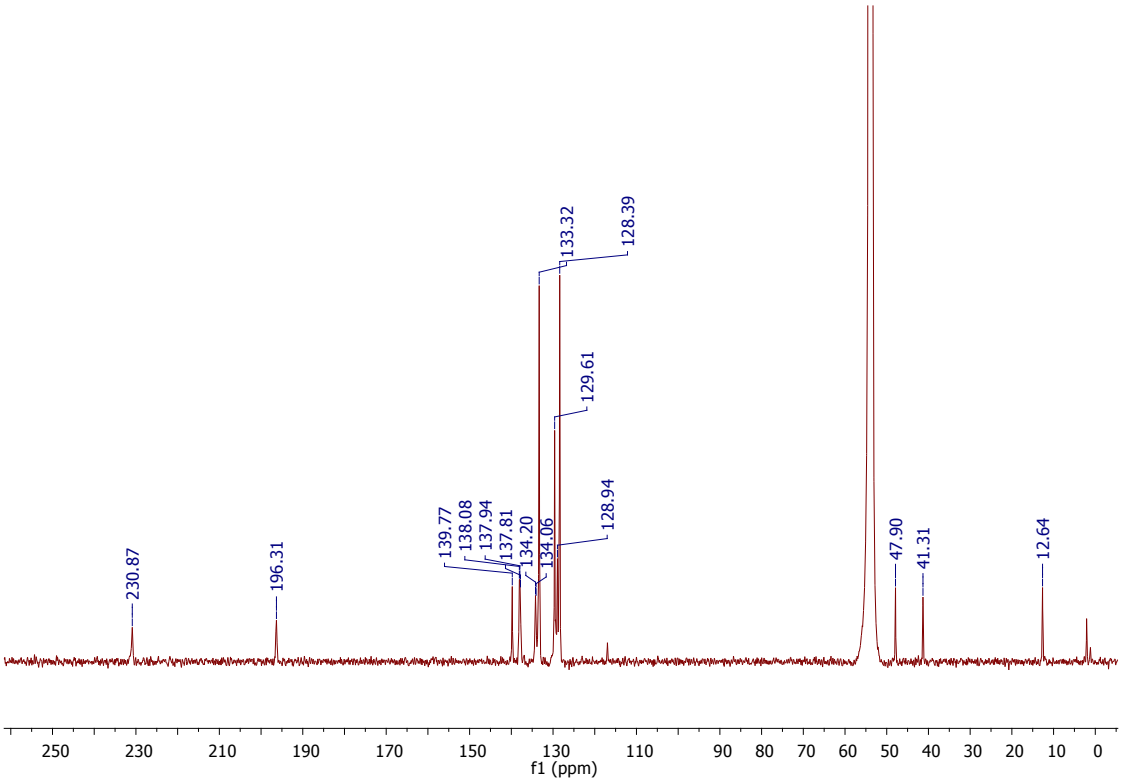

Figure S36. ^{13}C NMR spectrum (CD_2Cl_2, 500 MHz) of complex **11**.

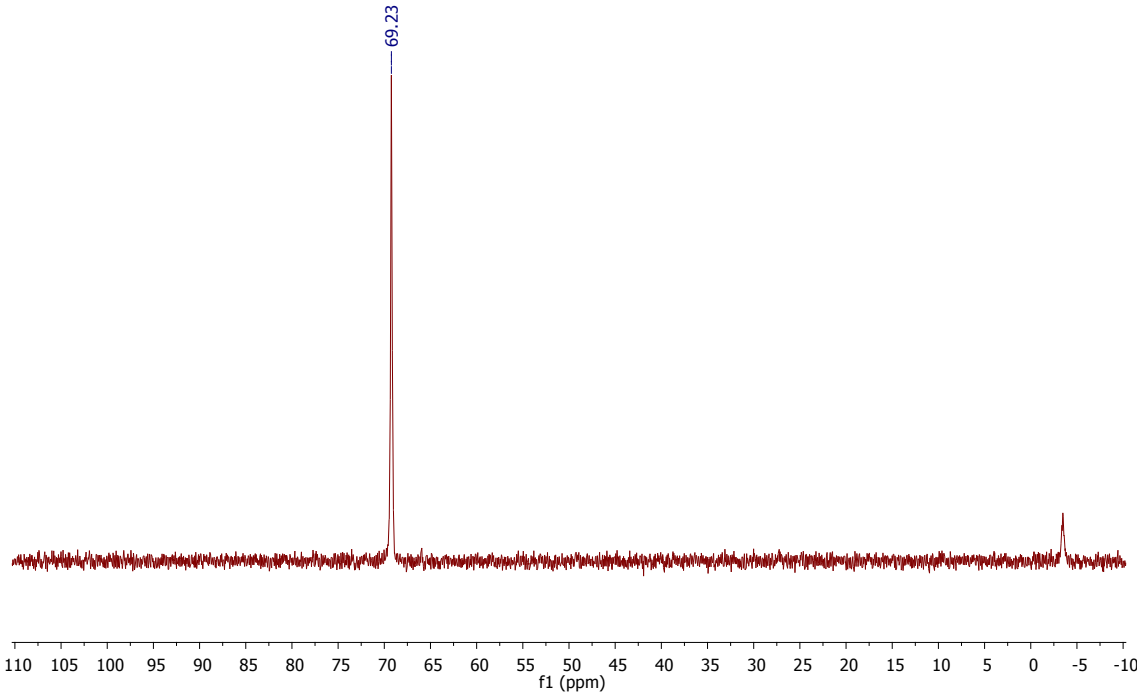

Figure S37. ^{31}P NMR (CD_2Cl_2, 400 MHz) of complex **11**.

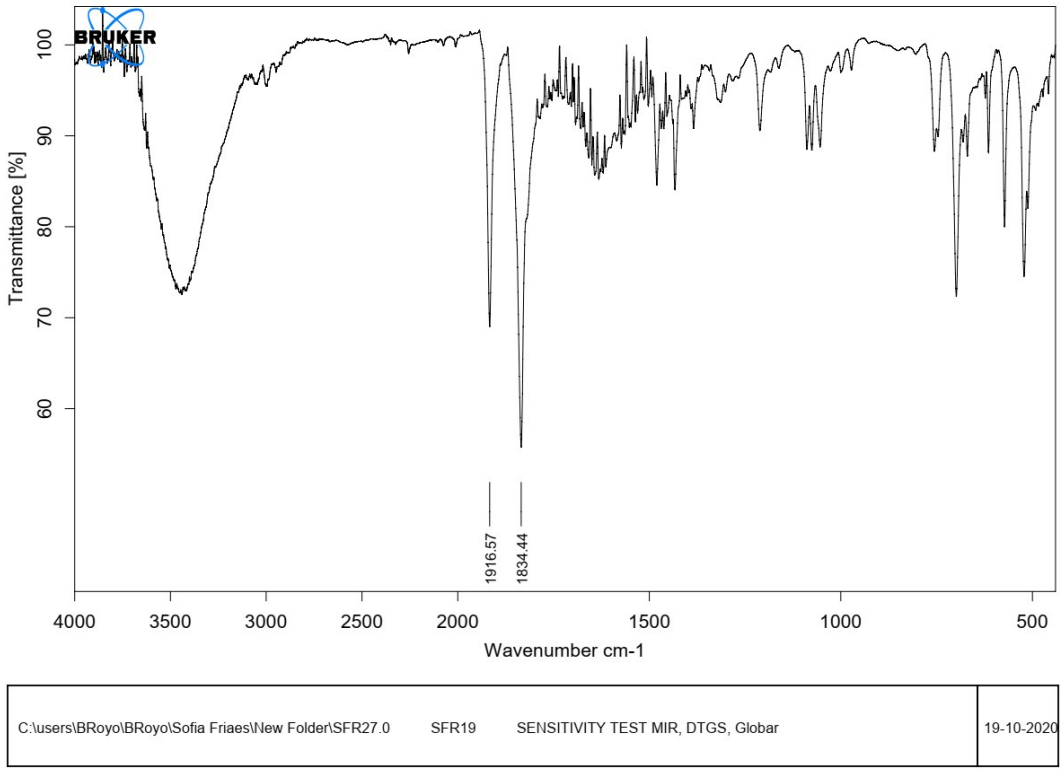

Figure S38. IR spectrum of compound **11** in KBr.

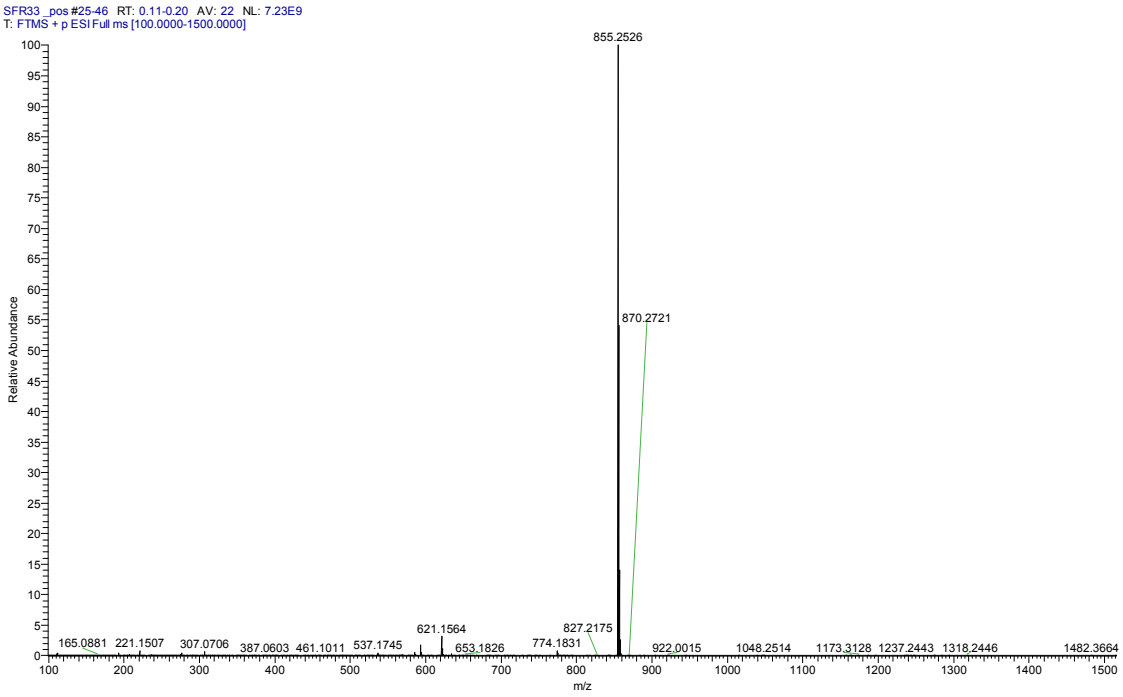

Figure S39. ESI-HRMS Spectrum of complex **11**.

4. NMR spectra of the reactions of **2** and **9** with PPh_3

a)

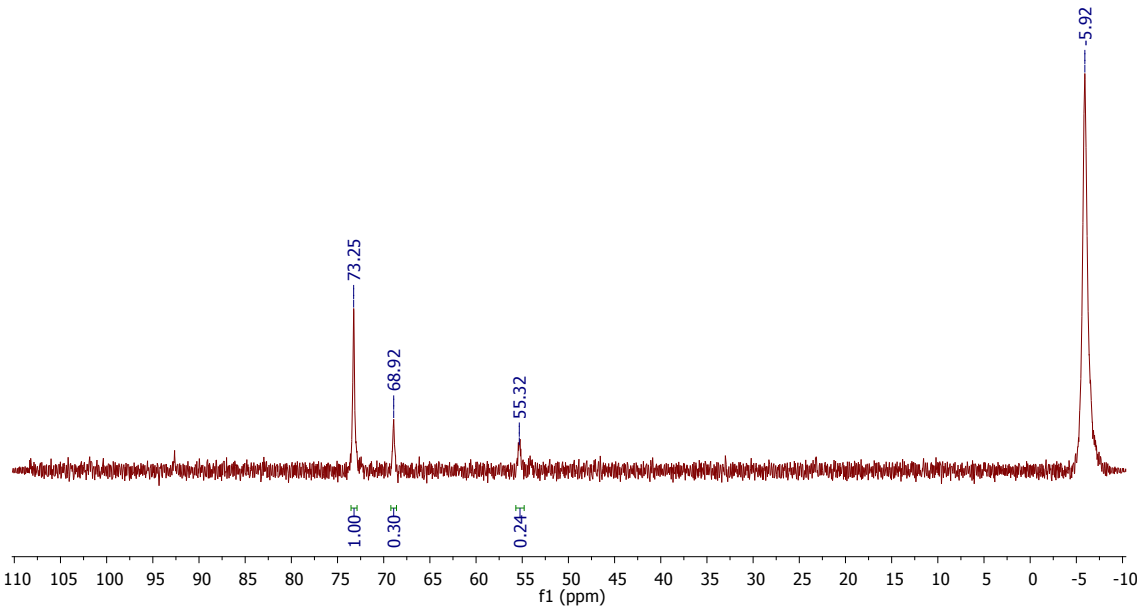

b)

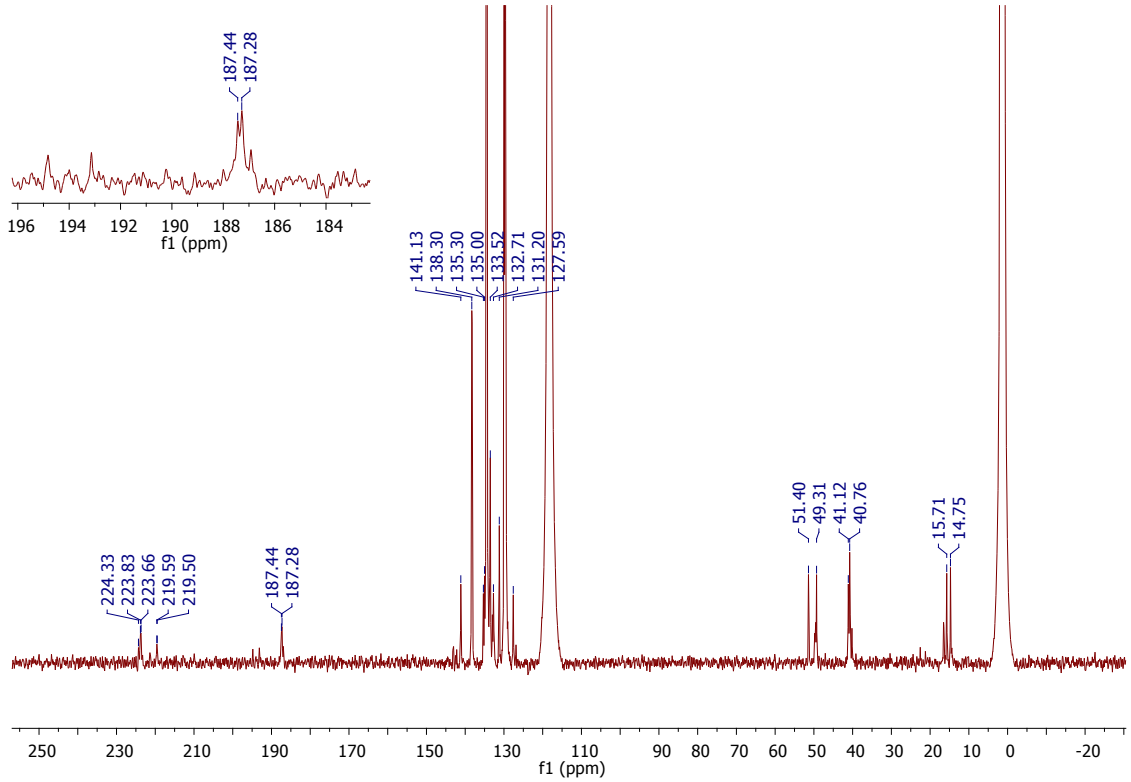

Figure S40. NMR spectra of the reaction mixture of complex **9** with 1 eqv. PPh_3 under irradiation (violet light 380-450 nm, 9.5 W, LED) for 8 h. a) ^{31}P NMR (CD_3CN, 400 MHz) b) ^{13}C NMR (CD_3CN, 500 MHz).

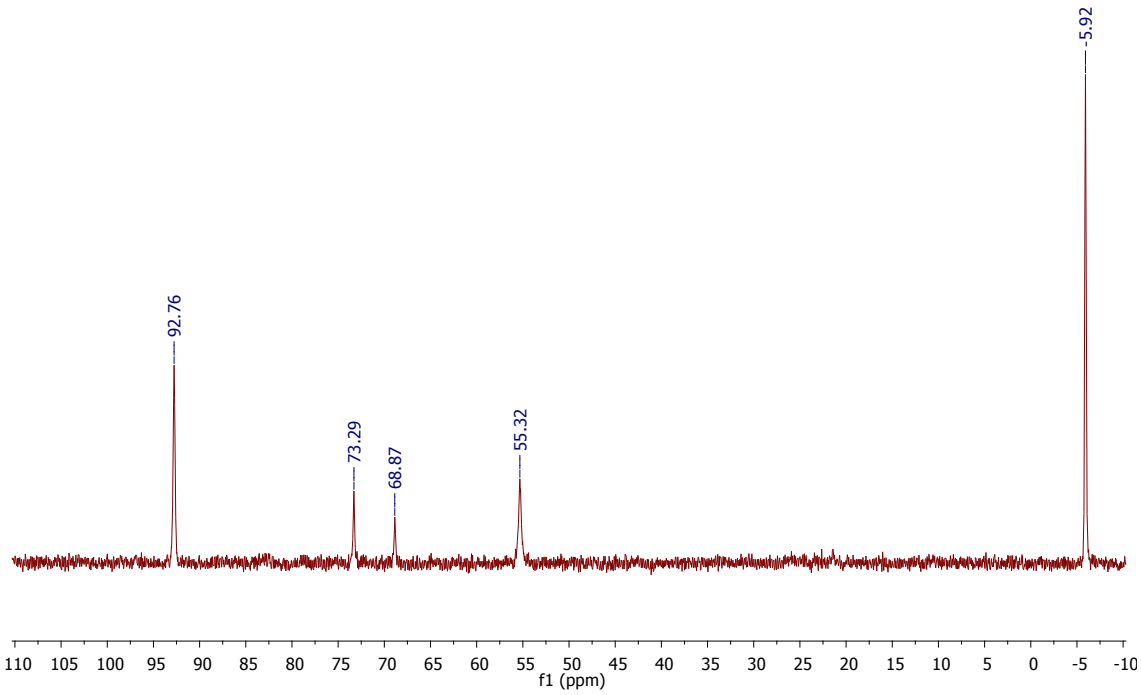

Figure S41. ^{31}P NMR (CD_3CN, 400 MHz) of the reaction of complex **2** with 2 eqv. PPh_3 under irradiation (violet light 380-450 nm, 9.5 W, LED)for 3 days.

5. Electrochemical studies: cyclic voltammetry of complexes **1-10** and infrared spectroelectrochemistry of complex **9**.

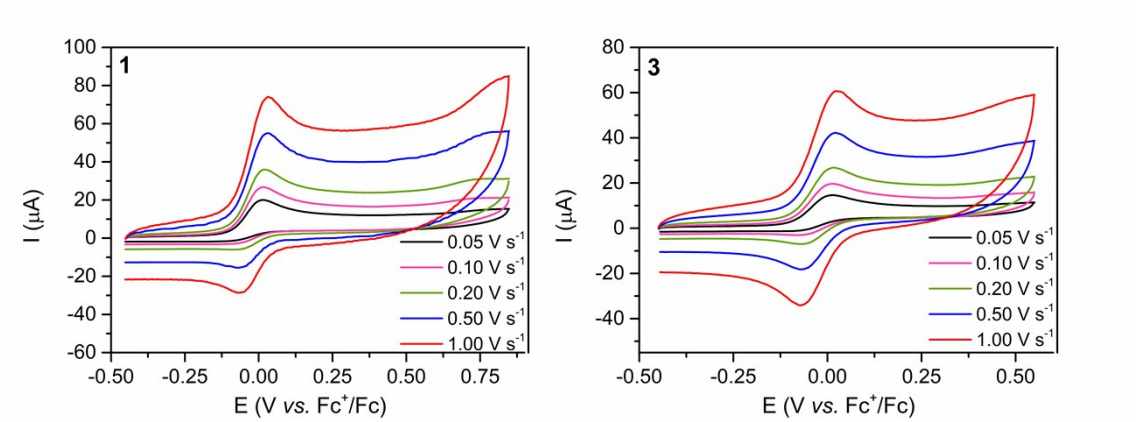

Figure S42. Cyclic voltammograms in the anodic region of complexes **1** and **3** (1 mM) in CH_3CN, N_2 saturated solutions using $TBAPF_6$ as supporting electrolyte (0.1 M) at different scan rates within [-0.45; 0.85] V *vs*. Fc^+/Fc. Glassy carbon (3 mm diameter) was used as working, platinum wire as counter and 3M Ag/AgCl as reference electrodes.

Table S1. Electrochemical data in the anodic region for **1** in solution at different scan rates.

Scan rate ($V\ s^{-1}$)	I_p^a (mA)	I_p^c (mA)	$\lvert I_p^c/I_p^a \rvert$	E_p^a (V)	E_p^c (V)	ΔE (V)	$E_{1/2}$ (V)
0.05	18.17	-	-	0.01	-	-	-0.06
0.10	23.95	-0.47	0.020	0.01	-0.06	0.075	-0.06
0.20	31.55	-3.87	0.123	0.02	-0.05	0.070	-0.06
0.50	45.78	-13.55	0.296	0.03	-0.06	0.080	-0.06
1.00	56.74	-20.83	0.367	0.03	-0.05	0.087	-0.06

Table S2. Electrochemical data in the anodic region for **3** in solution at different scan rates.

Scan rate ($V\ s^{-1}$)	I_p^a (mA)	I_p^c (mA)	$\lvert I_p^c/I_p^a \rvert$	E_p^a (V)	E_p^c (V)	ΔE (V)	$E_{1/2}$ (V)
0.05	12.59	-	-	0.01	-	-	-0.05
0.10	17.42	-6.04	0.346	0.01	-0.06	0.050	-0.05
0.20	22.26	-9.91	0.445	0.02	-0.05	0.030	-0.05
0.50	32.87	-18.52	0.563	0.02	-0.07	0.050	-0.04
1.00	43.08	-28.54	0.662	0.03	-0.09	0.060	-0.04

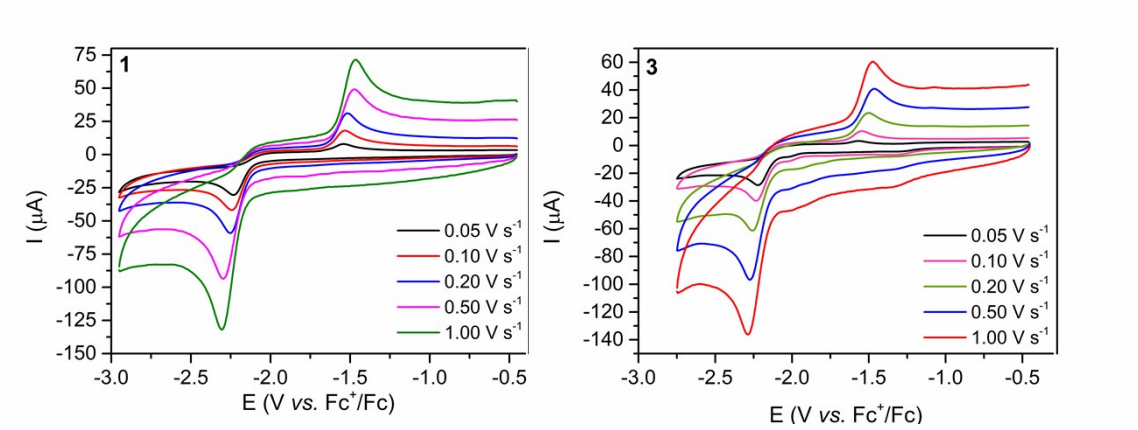

Figure S43. Cyclic voltammograms in the cathodic region of complexes **1** and **3** (1 mM) in CH_3CN, N_2 saturated solutions using $TBAPF_6$ as supporting electrolyte (0.1 M) at different scan rates within [-2.95; -0.45] V *vs*. Fc^+/Fc for **1** and [-2.75; -0.45] V *vs*. Fc^+/Fc for **3**. Glassy carbon (3 mm diameter) was used as working, platinum wire as counter and 3M Ag/AgCl as reference electrodes.

Table S3. Electrochemical data in the cathodic region for **1** in solution at different scan rates.

Scan rate ($V\ s^{-1}$)	I_p^a (mA)	I_p^c (mA)	$\lvert I_p^c/I_p^a \rvert$	E_p^a (V)	E_p^c (V)	ΔE (V)	$E^c_{1/2}$ (V)
0.05	6.27	-25.16	0.249	-1.54	-2.22	0.685	-2.17
0.10	13.98	-32.36	0.432	-1.53	-2.34	0.701	-2.17
0.20	25.57	-46.67	0.548	-1.52	-2.24	0.724	-2.18
0.50	37.62	-72.81	0.517	-1.474	-2.29	0.812	-2.22
1.00	54.01	-97.07	0.556	-1.464	-2.30	0.836	-2.23

Table S4. Electrochemical data in the cathodic region for **3** in solution at different scan rates.

Scan rate ($V\ s^{-1}$)	I_p^a (mA)	I_p^c (mA)	$\lvert I_p^c/I_p^a \rvert$	E_p^a (V)	E_p^c (V)	ΔE (V)	$E^c_{1/2}$ (V)
0.05	2.61	-20.32	0.128	-1.57	-2.22	0.650	-2.15
0.10	6.97	-27.09	0.257	-1.54	-2.23	0.690	-2.16
0.20	15.50	-42.12	0.367	-1.50	-2.26	0.760	-2.18
0.50	25.93	-62.45	0.415	-1.47	-2.27	0.800	-2.19
1.00	38.0	-88.03	0.432	-1.48	-2.29	0.810	-2.20

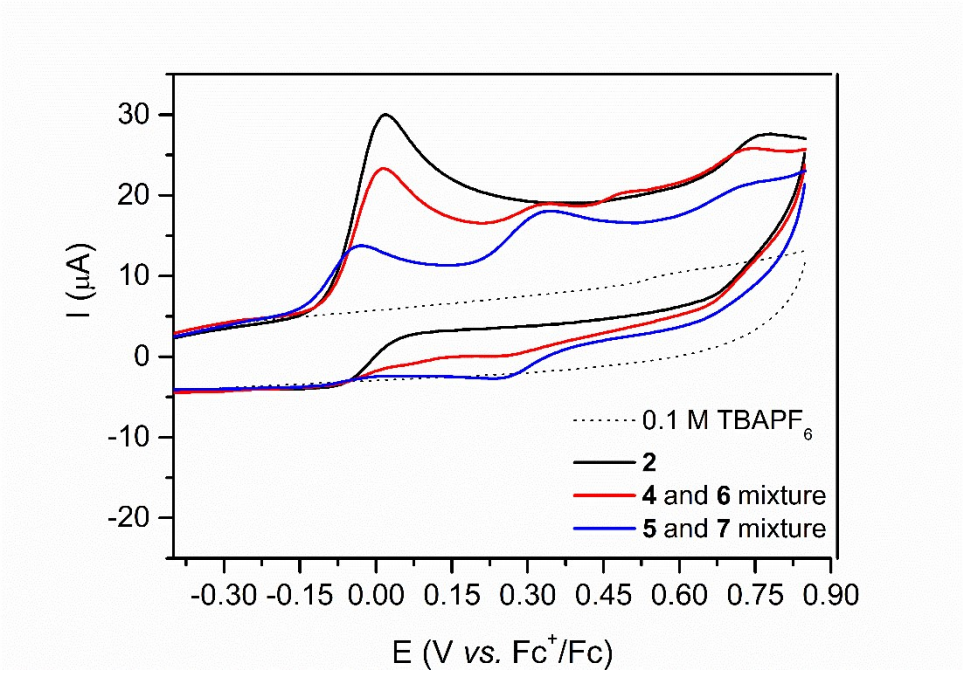

Figure S44. Cyclic voltammograms of complexes **2, 4, 6, 5** and **7** (1 mM) in CH_3CN, N_2 saturated solutions using $TBAPF_6$ as supporting electrolyte (0.1 M) at 0.10 V s^{-1}. Glassy carbon (3 mm diameter) was used as working, platinum wire as counter and 3M Ag/AgCl as reference electrodes.

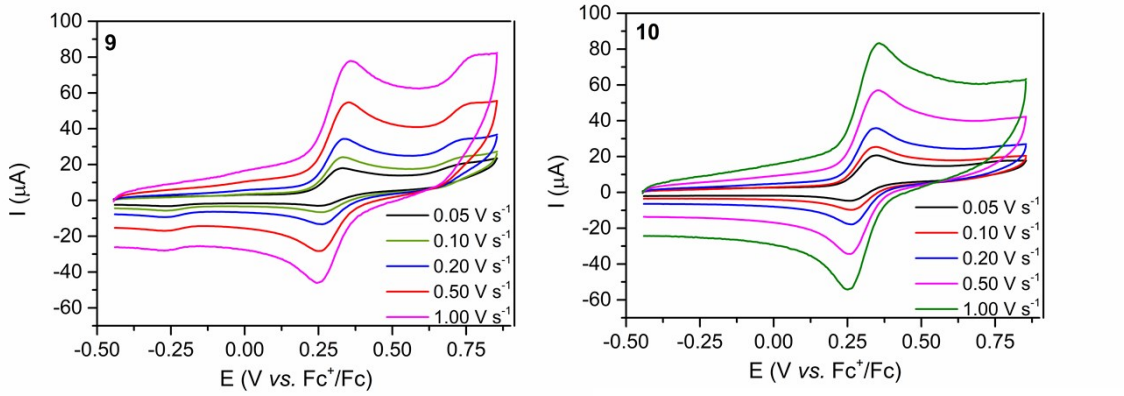

Figure S45. Cyclic voltammograms in the anodic region of complexes **9** and **10** (1 mM) in CH_3CN, N_2 saturated solutions using $TBAPF_6$ as supporting electrolyte (0.1 M) at different scan rates within [-0.45; 0.85] V *vs*. Fc^+/Fc. Glassy carbon (3 mm diameter) was used as working, platinum wire as counter and 3M Ag/AgCl as reference electrodes.

Table S5. Electrochemical data in the anodic region for **9** in solution at different scan rates.

Scan rate (V s^{-1})	I_p^a (mA)	I_p^c (mA)	$\lvert I_p^c/I_p^a \rvert$	E_p^a (V)	E_p^c (V)	ΔE (V)	$E_{1/2}$ (V)
0.05	14.30	-5.61	0.392	0.32	-0.27	0.05	0.24
0.10	19.97	-8.21	0.411	0.32	-0.26	0.06	0.24
0.20	25.95	-12.32	0.475	0.32	-0.27	0.05	0.24
0.50	39.02	-21.73	0.557	0.34	-0.27	0.07	0.24
1.00	52.03	-31.70	0.609	0.35	-0.27	0.08	0.02

Table S6. Electrochemical data in the anodic region for **10** in solution at different scan rates.

Scan rate ($V\ s^{-1}$)	I_p^a (mA)	I_p^c (mA)	$\lvert I_p^c/I_p^a \rvert$	E_p^a (V)	E_p^c (V)	ΔE (V)	$E^c_{1/2}$ (V)
0.05	16.89	-8.45	0.500	0.34	-0.27	0.070	0.26
0.10	20.98	-11.81	0.563	0.34	-0.27	0.070	0.26
0.20	28.66	-16.87	0.589	0.33	-0.27	0.060	0.25
0.50	43.54	-29.53	0.678	0.34	-0.27	0.070	0.25
1.00	58.99	-43.38	0.735	0.35	-0.26	0.090	0.23

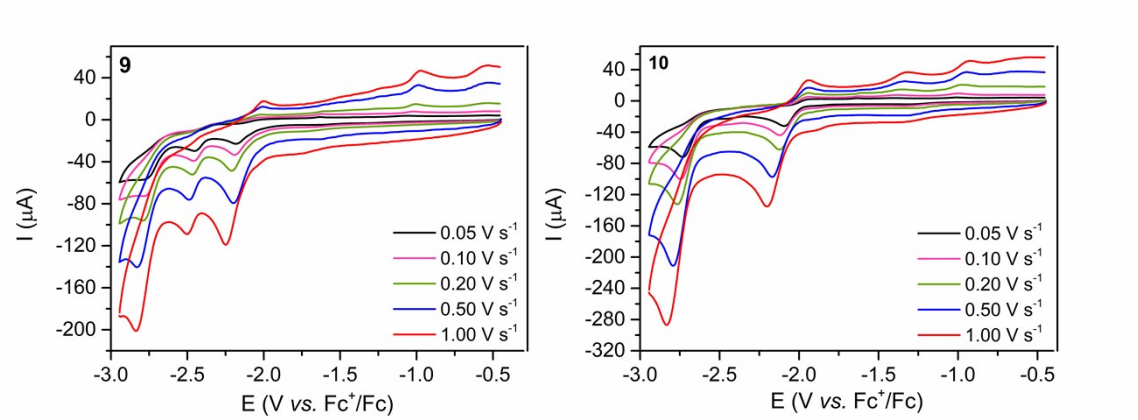

Figure S46. Cyclic voltammograms in the cathodic region of complexes **9** and **10** (1 mM) in CH_3CN, N_2 saturated solutions using $TBAPF_6$ as supporting electrolyte (0.1 M) at different scan rates within [-2.95; -0.45] V *vs.* Fc^+/Fc. Glassy carbon (3 mm diameter) was used as working, platinum wire as counter and 3M Ag/AgCl as reference electrodes.

Table S7. Electrochemical data in the cathodic region for **9** in solution at different scan rates.

Scan rate ($V\ s^{-1}$)	I_p^{c1} (mA)	I_p^{c2} (mA)	I_p^{a1} (mA)	E_p^{c1} (V)	E_p^{c2} (V)	E_p^{a1} (V)	$E^{c1}_{1/2}$ (V)
0.05	-13.22	-7.97	-	-2.18	-2.45	-	-2.12
0.10	-20.56	-11.51	-	-2.18	-2.45	-	-2.11
0.20	-30.85	-21.04	-	-2.20	-2.46	-	-2.14
0.50	-51.40	-20.36	7.08	-2.19	-2.48	-2.00	-2.12
1.00	-78.58	-19.47	4.42	-2.24	-2.50	-2.01	-2.17

Table S8. Electrochemical data in the cathodic region for **10** in solution at different scan rates.

Scan rate ($V\ s^{-1}$)	I_p^{c1} (mA)	I_p^{c2} (mA)	I_p^{a1} (mA)	E_p^{c1} (V)	E_p^{c2} (V)	E_p^{a1} (V)	$E^{c1}_{1/2}$ (V)
0.05	-23.87	-46.31	-	-2.09	-2.72	-	-2.04
0.10	-33.26	-64.63	9.37	-2.11	-2.74	-1.96	-2.05
0.20	-48.6	-83.33	11.14	-2.11	-2.75	-1.95	-2.05
0.50	-74.19	-130.36	18.76	-2.16	-2.78	-1.95	-2.09
1.00	-102.97	-174.28	30.25	-2.20	-2.82	-1.95	-2.11

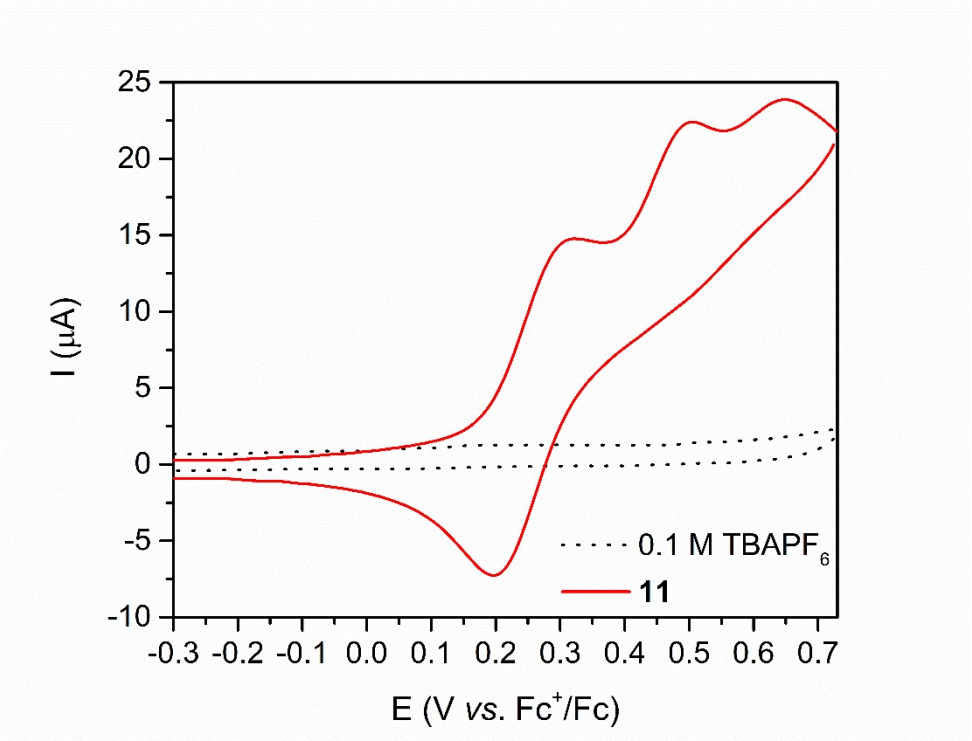

Figure S47. Cyclic voltammogram of complex **11** (1 mM) in CH_2Cl_2, N_2 saturated solutions using $TBAPF_6$ as supporting electrolyte (0.1 M) at 0.10 V s^{-1}. Glassy carbon (3 mm diameter) was used as working, platinum wire as counter and 3M Ag/AgCl as reference electrodes.

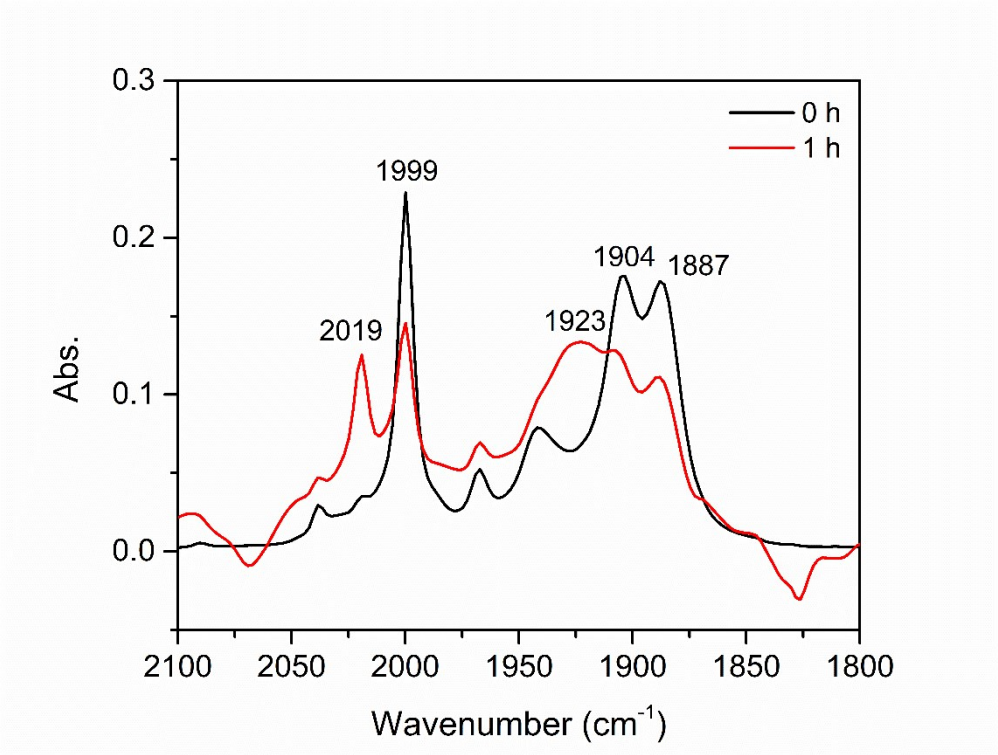

Figure S48. FTIR spectra of **9** in a 5 mM acetonitrile solution recorded under N_2 atmosphere after dissolving **9** (0 h) in black, and after 1 h in solution in red. The background spectra were obtained in acetonitrile. A slow solvolysis equilibrium between the neutral starting species **9** (vCO = 1999, 1904 and 1887 cm^{-1}) and $[Mn(CO)_3(di\text{-}trz^{Et})(CH_3CN)]^+$ (**$9CH_3CN^+$**,vCO = 2019, 1923 (broad resonance) cm^{-1} occurs when **9** is dissolved in acetonitrile.

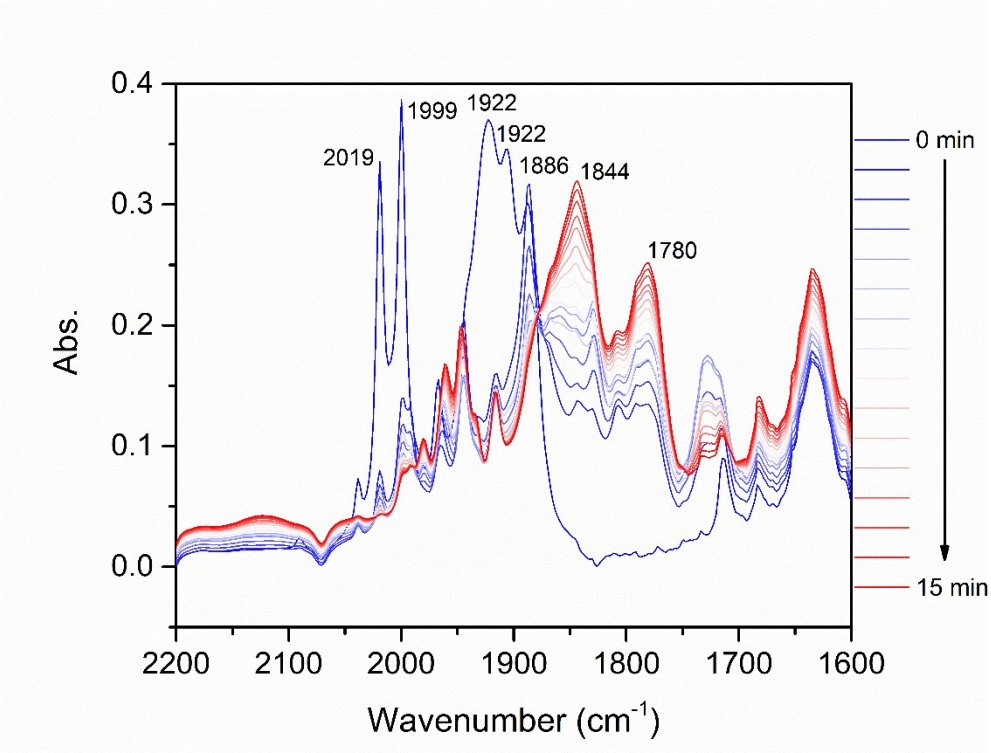

Figure S49. FTIR-SEC experiments during second reduction (at *ca.* -2.4 V) using 5 mM of **9** and 0.1 M $TBAPF_6$ in a N_2 saturated CH_3CN solution, Pt grids as working and counter electrodes and Ag wire as pseudo-reference electrode. Blue spectrum corresponds to 0 min. and red after the 15 min. of experiment.

6. DFT calculations for complex **9**

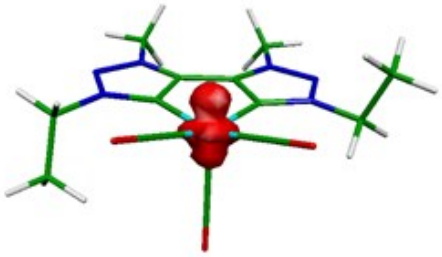

Figure S50. DFT calculated spin density of reduction intermediate **9'**.

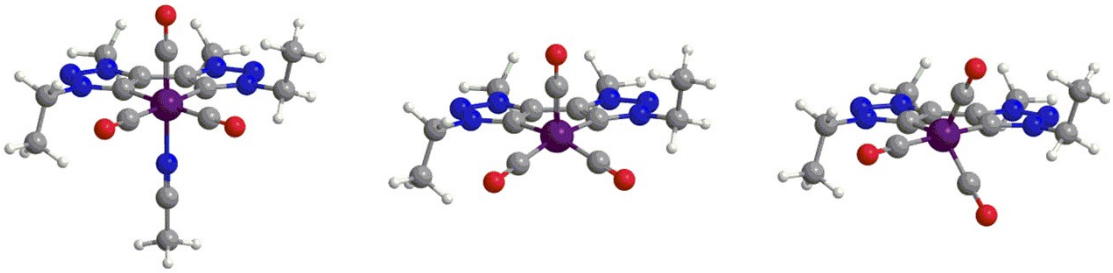

Figure S51. DFT optimized geometry of the reduction intermediates.

Atomic coordinates of the optimized geometries

[Mn(CO)$_3$(trz^{Et})Br] (9)

Mn	0.109007	-0.546572	0.715054
Br	-0.026415	-2.709521	-0.719438
N	-1.914456	1.299308	-2.403778
N	-2.643598	0.420323	-0.655662
N	2.556483	0.371211	-1.174310
N	1.512783	1.268265	-2.744871
N	-3.031985	1.026687	-1.767856
C	1.471207	-1.321988	1.587933
N	2.728439	0.973468	-2.341947
C	0.590599	0.860638	-1.842165
C	3.760219	-0.036024	-0.454112
C	-1.065970	-1.319606	1.828900
H	5.026222	0.616361	1.149249
H	3.323089	1.064304	1.363067
C	4.127757	0.960845	0.629090
C	-1.301518	0.263762	-0.527838
H	-4.535181	0.629397	0.136648
H	-3.302169	0.030709	1.255092
H	-4.846583	-1.825883	0.628544
H	-3.228980	-2.153608	-0.035322
C	-3.692966	-0.057769	0.240645
C	0.193887	0.938771	1.647907
C	-4.093080	-1.484534	-0.087238
C	-0.839938	0.869049	-1.702990
C	1.264263	0.249722	-0.777690
H	-4.520225	-1.543354	-1.093088
H	4.334576	1.944020	0.195444
H	4.553111	-0.123431	-1.199384
H	3.566834	-1.027646	-0.042823
C	1.363856	1.934329	-4.027123
H	2.362416	2.081893	-4.435624
H	0.874583	2.898452	-3.883088
H	0.775782	1.307293	-4.698542
C	-2.007036	1.987990	-3.679865
H	-1.577964	1.362610	-4.463726
H	-1.476658	2.939208	-3.621052
H	-3.063085	2.162196	-3.879822
O	2.313408	-1.843684	2.188205
O	0.240563	1.931068	2.250841
O	-1.779178	-1.837457	2.580437

[Mn(CO)$_3$(trz^{Et})(CH$_3$CN)]$^+$ (9CH$_3$CN$^+$)

Mn	0.151093	-0.955823	1.577155
N	-1.846758	0.906640	-1.556366
N	-2.594869	0.050116	0.195204
N	2.617674	-0.057296	-0.314952
N	1.580281	0.846527	-1.886207
N	-2.967130	0.663875	-0.915873
C	1.515446	-1.646255	2.528495
N	2.792563	0.554248	-1.474775
C	0.652334	0.425986	-0.994484
C	3.820156	-0.458653	0.413764
C	-1.032763	-1.608489	2.766757
H	5.088319	0.217718	2.003486
H	3.388881	0.684963	2.206253
C	4.193194	0.558639	1.475555
C	-1.256805	-0.136172	0.318598
H	-4.484706	0.312360	0.969612
H	-3.270312	-0.269048	2.115558
H	-4.866510	-2.103292	1.523186
H	-3.245793	-2.508492	0.926124
C	-3.655802	-0.385569	1.101941
C	0.250289	0.607850	2.419686
C	-4.083178	-1.813212	0.817179
C	-0.781084	0.449490	-0.857891
C	1.322870	-0.183002	0.069773
H	-4.482228	-1.901897	-0.197655
H	4.408615	1.530052	1.020493
H	4.611145	-0.565838	-0.330781
H	3.620334	-1.441499	0.842765
C	1.440472	1.526423	-3.163184
H	2.442142	1.673519	-3.563868
H	0.954721	2.490866	-3.010283
H	0.853512	0.907823	-3.842998
C	-1.927579	1.594656	-2.834729
H	-1.495831	0.965142	-3.613412
H	-1.393689	2.543582	-2.772174
H	-2.981746	1.772416	-3.040859
O	2.353148	-2.095100	3.185688
O	0.305085	1.639921	2.936696
O	-1.747320	-2.031736	3.570148
N	0.024615	-2.626909	0.466903
C	-0.040510	-3.590049	-0.167812
C	-0.121854	-4.794814	-0.963169
H	-0.113280	-5.669529	-0.306943
H	-1.047097	-4.789268	-1.545880
H	0.733153	-4.844875	-1.643124

[Mn(CO)$_3$(trz^{Et})] (9')

Mn	0.140369	-0.463425	0.762307
N	-1.902216	1.243913	-2.434874
N	-2.625941	0.438118	-0.649787
N	2.578076	0.416485	-1.165379
N	1.525040	1.239646	-2.770002
N	-3.016672	1.008614	-1.778468
C	1.447062	-1.472266	1.421041
N	2.744372	0.995371	-2.343945
C	0.604260	0.822726	-1.869652
C	3.785295	0.078785	-0.415839
C	-1.021219	-1.435650	1.695305
H	5.002564	0.828158	1.182848
H	3.276206	1.184767	1.378152
C	4.090481	1.114243	0.650918
C	-1.279889	0.271264	-0.520945
H	-4.465519	0.769264	0.223787
H	-3.233679	0.051146	1.275031

H	-4.971832	-1.644988	0.661908
H	-3.401182	-2.110165	-0.017409
C	-3.673432	0.019005	0.277428
C	0.282769	0.860478	1.932617
C	-4.199571	-1.364053	-0.060034
C	-0.825912	0.825647	-1.729403
C	1.281541	0.260664	-0.775347
H	-4.641667	-1.377408	-1.060799
H	4.247430	2.099609	0.201401
H	4.594395	0.009275	-1.145568
H	3.626670	-0.908831	0.019569
C	1.372031	1.870060	-4.069638
H	2.370078	2.021856	-4.477909
H	0.868009	2.830396	-3.953124
H	0.796139	1.217195	-4.726783
C	-1.998502	1.890611	-3.732380
H	-1.556962	1.246878	-4.494042
H	-1.481397	2.850561	-3.701856
H	-3.055847	2.043833	-3.942488
O	2.272542	-2.151265	1.896802
O	0.374557	1.723821	2.715771
O	-1.739713	-2.088107	2.347691

[Mn(CO)$_3$(trz^{Et})] ([9′]$^-$)

Mn	0.062940	-0.337087	0.833807
N	-1.928707	1.241413	-2.459525
N	-2.673240	0.404404	-0.694968
N	2.511806	0.497618	-1.041071
N	1.520671	1.293604	-2.699733
N	-3.052158	0.955950	-1.842707
C	0.985044	-1.822847	0.864066
N	2.724370	1.044574	-2.231305
C	0.560880	0.914290	-1.820392
C	3.686959	0.142096	-0.255909
C	-1.144065	-0.995376	1.945779
H	5.056908	0.989846	1.164922
H	3.398084	1.596915	1.323600
C	4.167126	1.296518	0.606473
C	-1.309454	0.291330	-0.502564
H	-4.606818	0.570646	-0.005245
H	-3.399840	0.110823	1.208579
H	-4.857182	-1.837412	0.640931
H	-3.187237	-2.155756	0.137990
C	-3.735352	-0.060843	0.184342
C	0.765317	0.713606	2.038661
C	-4.062782	-1.526054	-0.044143
C	-0.853913	0.875009	-1.722302
C	1.196170	0.368991	-0.676352
H	-4.407929	-1.690552	-1.069818
H	4.431232	2.159539	-0.012796
H	4.461159	-0.171178	-0.960615
H	3.402712	-0.719354	0.351424
C	1.407463	1.885601	-4.018078
H	2.416121	2.036840	-4.400325
H	0.889493	2.843785	-3.948694
H	0.857529	1.212148	-4.678164
C	-2.001818	1.882917	-3.757896
H	-1.531513	1.247091	-4.510083
H	-1.496185	2.849436	-3.719275
H	-3.054823	2.024106	-3.997794
O	1.636669	-2.810013	0.950699
O	1.262831	1.348615	2.909136
O	-1.909733	-1.455002	2.716249

7. Crystallographic details of complexes **3**-**5**, **10** and **11** S30

Table S9. Crystallographic data and refinement details for structures **3**, **4**, **5**, **10** and **11**.

	3	**4**	**5**	**10**	**11**
Formula	$C_{20}H_{20}Mn_2N_6O_8$	$C_{22}H_{24}Mn_2N_6O_8$	$C_{28}H_{20}Mn_2N_6O_8$	$C_{28}H_{30}BrCl_2MnN_6O_3$	$C_{50}H_{51}BrMnN_7O_3P_2$
M	582.30	610.35	678.37	704.32	994.77
λ (Å)	0.71073	0.71073	0.71073	0.71073	0.71073
T (K)	110(2)	110(2)	110(2)	110(2)	110(2)
crystal system	Triclinic	Monoclinic	Orthorhombic	Monoclinic	Triclinic
space group	*P*-1	P21/n	Pbcn	P21/c	*P*-1
a (Å)	8.5189(11)	12.2841(6)	14.5175(8)	23.1550(19)	11.7228(19)
b (Å)	9.5568(12)	16.2240(8)	10.1261(8)	14.0329(12)	13.508(2)
c (Å)	16.277(2)	13.1914(6)	19.3690(10)	19.7444(18)	14.793(2)
α (°)	104.178(5)	90	90	90	90.963(6)
β (°)	91.950(5)	103.688(2)	90	103.759(3)	98.570(5)
γ (°)	106.855(4)	90	90	90	101.111(5)
V (Å^3)	1221.7(3)	2554.3(2)	2847.4(3)	6231.5(9)	2270.4(7)
Z	2	4	4	8	2
ρ_{calc} (g.cm^{-3})	1.583	1.587	1.582	1.501	1.455
μ (mm^{-1})	1.090	1.047	0.949	1.917	1.293
Crystal size	0.30x0.14x0.08	0.24x0.18x0.10	0.18x0.12x0.08	0.30x0.20x0.16	0.30x0.30x0.20
Crystal color	Yellow	Orange	Yellow	Orange	Yellow
Crystal description	Plate	Prism	Prism	Prism	Plate
θ_{max} (°)	25.678	44.215	37.861	29.203	25.350
total data	30202	125482	37470	90561	72752
unique data	4633	19991	7524	16765	8301
R_{int}	0.1754	0.1288	0.0977	0.1139	0.3020
R [I>2σ(I)]	0.0569	0.0591	0.0907	0.1127	0.1111
R_w	0.1015	0.1378	0.1567	0.1721	0.3019
Goodness of fit	1.022	0.950	1.138	1.185	1.139
ρ_{min}	-0.588	-1.613	-1.070	-1.359	-1.391
ρ_{max}	0.714	1.451	0.964	1.997	2.054

The data were deposited in the CCDC under deposit numbers 2060440 for **3**, 2060441 for **4**, 2060442 for **5** and 2060443 for **10**, and 2060444 for **11**.

X-Ray Structure of complex **11**

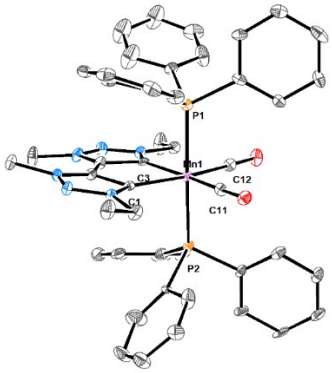

Figure S52. ORTEP-3 diagram of complex **11**, using 30% probability level ellipsoids. All hydrogen atoms, the Br- counter ion, one acetonitrile and a water molecule were omitted for clarity. Selected bond lengths: Mn1–P1 2.275(3) Å, Mn1–P2 2.287(3) Å, Mn1–C1 2.065(10) Å, Mn1–C3 2.032(10) Å, Mn1–C11 1.758(11) Å, Mn1–C12 1.790(11) Å.

8. FT-IR spectra of the reaction of $Mn(CO)_5Br$ with $KOBu^t$ and $LiOPr^i$

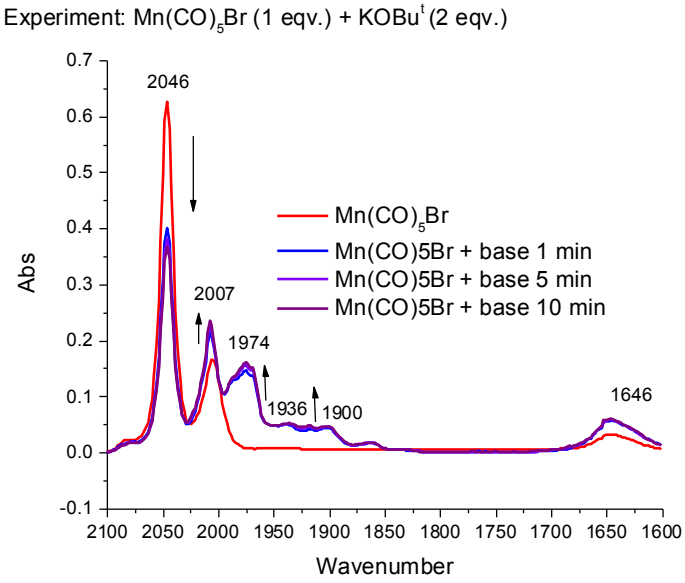

Figure S53. FTIR spectra of the reaction mixture of $Mn(CO)_5Br$ (1 eqv.) and $KOBu^t$ (2 eqv.) monitored during 10 min.

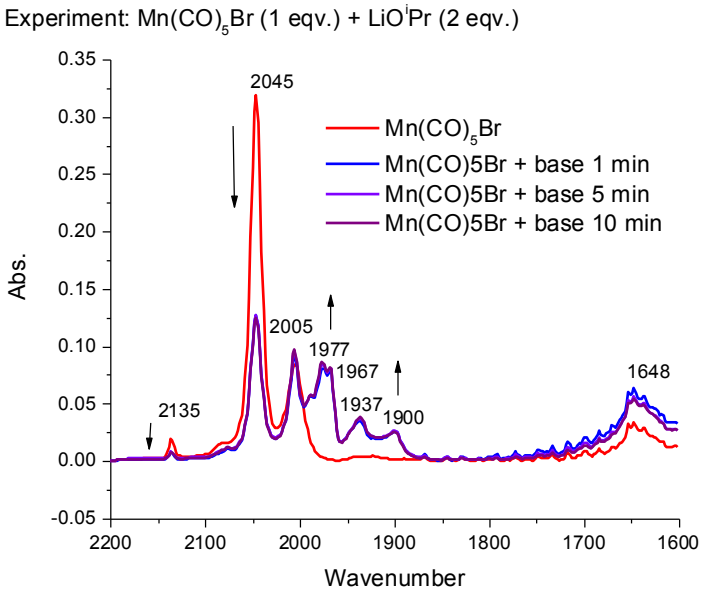

Figure S54. FTIR spectra of the reaction mixture of $Mn(CO)_5Br$ (1 eqv.) and $LiOPr^i$ (2 eqv.) monitored during 10 min.